Tissue and Cell 69 (2021) 101494

Contents lists available at ScienceDirect

Tissue and Cell

journal homepage: www.elsevier.com/locate/tice

Review

A systematic review of decellularized allograft and xenograft–derived scaffolds in bone tissue regeneration

Zahra Amini [a], Roya Lari [a,b,*]

[a] Department of Biology, Faculty of Science, Ferdowsi University of Mashhad, Mashhad, Iran
[b] Ferdowsi University of Mashhad, Faculty of Sciences, Institute of Applied Zoology, Research Department of Zoological Innovations (RDZI), Mashhad, Iran

ARTICLE INFO

Keywords:
Natural scaffold
Tissue engineering
Human
Animal
Biomaterials

ABSTRACT

Bone substitutes are used in nearly half of all musculoskeletal surgeries. The "gold standard" graft is an autograft that is limited by supply and site morbidity. Therefore, allograft sources are the current alternative for clinical practice with some side effects, such as immune responses and risk of disease transmission. In this paper, we have systematically reviewed the development and characterization of decellularized allograft or xenograft-derived scaffolds as bone graft substitutes. The databases of PubMed, Cochrane, Scopus, and Web of Science were searched for experimental studies that investigated the potential of acellular allograft or xenograft-derived scaffold for bone regeneration. The search was finalized on 14 September 2020. The initial electronic database search resulted in a total of 484 studies. During the screening process, 416 studies were excluded due to not meeting the inclusion criteria. Finally, a total of 68 articles were included, in which human or animal tissues have been decellularized for bone tissue generation purposes. Although in most studies, a decellularized bone was used for the generation of a bone scaffold, other decellularized tissues, such as the human amniotic membrane or human adipose tissue, were also used in some researches for this purpose. In 42 studies out of the 68, decellularized bone scaffolds were implanted into *in vivo* animal models. 8 studies used animal bone tissues as an allograft. 12 studies used human tissues as a xenograft. The studies have shown that decellularized allograft or xenograft scaffolds have high biocompatibility with little or no host response, and can enhance new bone formation. Overall, the results of this study suggest that the decellularized xenograft-derived cancellous bone scaffolds can be considered as alternatives to the autologous bone graft. This systematic review might affect future research directions and the preoperative planning of graft selection.

1. Introduction

Bone is a tissue with an excellent ability to repair fractures or breakages by natural mechanisms (Sikavitsas et al., 2001), yet severe bone injuries that may be caused by trauma, tumor, pathological degeneration, or congenital deformations are significant therapeutics issues and cannot be restored by conventional repair mechanisms (Ho-Shui-Ling et al., 2018). Bone grafts or bone substitutes are used in nearly half of all orthopedic surgeries, that required to have osteoconductive, osteoinductive, and osteogenic properties to provide support for bone regeneration (Konofaos et al., 2014; Raghuram et al., 2019). Currently, the main available grafts for patients suffering from slow or incomplete bone healing are either autologous or allograft (Ho-Shui-Ling et al., 2018). The autologous bone graft has been known as the "gold standard" that has osteoinductive and osteogenic properties, without immune response and the risk of disease transmission; it allows vascularization and new bone formation (Bhumiratana et al., 2016; Calori et al., 2011; Roddy et al., 2018). However, this graft is restricted by anatomical limitations, donor site morbidity, and pain (Lin et al., 2016). Allogeneic grafts are limited by their availability (Lin et al., 2016) and due to presence of cellular components (antigens), they increase the risks of immune reaction, abnormal remodeling, and failure to integrate within host tissue (Ma et al., 2013; Nie and Wang, 2018). Xenograft bone transplantation has been abandoned in orthopedic applications because of its failure to integrate with host tissues and extensive graft rejection (Roddy et al., 2018).

In recent years, bone tissue engineering has been suggested as an alternative for bone graft (Qing et al., 2019) and emerged to solve the problems of bone graft limitations, immune rejection, and pathogen transfer (Kon et al., 2018). The production of a tissue-engineered bone

* Corresponding author at: Department of Biology Faculty of Science, Ferdowsi University of Mashhad, 9177948974, Mashhad, Iran.
E-mail address: rlari@um.ac.ir (R. Lari).

https://doi.org/10.1016/j.tice.2021.101494
Received 2 August 2020; Received in revised form 9 January 2021; Accepted 10 January 2021
Available online 16 January 2021
0040-8166/

graft is depended on finding a biocompatible scaffold that accelerate cell homing, vascularization, and bone regeneration (Ho-Shui-Ling et al., 2018). There is a severe struggle to find the appropriate scaffold for bone tissue engineering. The scaffolds including autologous bone, allograft bone, xenograft bone, and a variety of biosynthetic grafts have been introduced; each has its own advantages and disadvantages and none is ideal (Liu and Lv, 2018). Among them, the decellularized bone scaffold has raised a lot of attention in bone tissue engineering, due to its ability for providing a natural biochemical environment, availability, and also lack of immunogenicity in host tissue (Mishra et al., 2016; Roseti et al., 2017). Additionally, the bioactive molecules such as growth factors and cytokines, conceivably maintain in the decellularized bone matrix (Chen and Lv, 2017). Hence, the extracellular matrix (ECM)-based scaffolds have been suggested as the most similar scaffold to the original tissue with osteoinductive properties (Ghassemi et al., 2018). The purpose of decellularization is to remove the genetic materials such as DNA and cellular component of native cells to prevent immune reactions while preserving its structural, biomechanical and biochemical properties (Benders et al., 2013). Cell-free natural ECMs can provide an appropriate microenvironment for differentiation of stem cells and proper molecular composition for bone development (Abedin et al., 2018; Schenke-Layland and Nerem, 2011; Tapias and Ott, 2014).

One of the most widely used bone scaffolds is the human decellularized bone matrix that can be obtained from surgery or cadavers, which has been shown to have both osteoconductive and osteoinductive potential (Gruskin et al., 2012). The human decellularized bone matrix can be used with appropriate growth factors to conduct better regeneration (Armiento et al., 2018). Although decellularized bone allografts display great potential for bone regeneration, their applications are restricted due to the limited availability and expensive cost of human tissues (Pirnay et al., 2015). Therefore, researchers may use a xenograft–derived scaffold that retained osteoconductive properties (Bracey et al., 2018). The availability, low cost, unlimited quantities, and less human disease transmission are the advantages of xenograft-derived bone scaffolds (Bracey et al., 2019a). Studies reported that a bone scaffold could be derived from xenograft and used for clinical orthopedic implants if, 1) devoid of cytotoxic processing chemicals, 2) lack of risk of viral or bacterial pathogen transmission, 3) reduced the immune response, and risk of rejection (Bracey et al., 2019b; He et al., 2020b; Seyler et al., 2017).

This study aimed to perform a systematic review of the literature about the use of decellularized xenograft and allograft-derived bone scaffolds as a bone graft, detailing the different decellularization protocols, the method for recellularization, and *in vivo* implantation.

2. Methods

The protocol for this systematic review was performed according to the statements and guidelines of the preferred reporting items of systematic reviews and meta-analyses (PRISMA) (Moher et al., 2015). This systematic review aimed to answer the following PICO question: "can acellular allogeneic or xenogeneic bone scaffolds be considered as a substitute for the bone graft and facilitate bone regeneration without any risk of rejection?". Four electronic databases of PubMed, Cochrane, Scopus, and Web of Science were systematically searched by authors without any limitations from inception up to September 14th, 2020 (Appendix 1). The search keywords were: "decellularized" or "acellular" AND "scaffold" AND "bone" or "bone graft" or "mineralization". The duplicate articles were deleted. The criteria were evaluated first by the titles and abstracts by authors independently. When the study met the inclusion criteria or if the title and abstract did not provide enough information, full articles were investigated. The conflicts were resolved by group discussion until a mutual consensus was reached. Details were extracted regarding publication information, sample type (i.e. human, animal, and cell), study design (*in vivo* or *in vitro*), and outcomes of the decellularized scaffolds.

Inclusion criteria:

1) Studies that used the natural tissue for the production of decellularized bone scaffolds.
2) Studies that used human tissues or animal tissues for the production of allograft or xenograft-derived scaffold.
3) Animal or human studies, which have been used in the bone repair or bone regeneration.

Exclusion criteria:

1) Studies that used scaffolds for another tissue engineering than bone
2) Studies that used hybrid scaffold (synthesis scaffold + natural bone)
3) Studies that used synthesis scaffold
4) Literature reviews
5) Unpublished and unavailable literature
6) Duplicate literature

In this paper, *in vitro* and *in vivo* studies were contemplated. No clinical trial that met the inclusion criteria was found. We could not perform a meta-analysis due to incomplete and wide heterogeneity of research data. So, the results were expressed descriptively.

3. Results

The initial electronic database search resulted in a total of 484 citations. 337 reports were excluded through title or/and abstract screening, 5 reports were unavailable, respectively (Appendix 1). 142 potentially relevant studies were selected for full-text review. 68 studies were identified in our systematic search. A flowchart of the search procedure can be found in Fig. 1.

3.1. Study characteristics

In vitro evaluation, which is often used to assess the biocompatibility, mineralization, and cytotoxicity of the decellularized scaffold is necessary for the estimation of material properties. 57 studies out of 68 analyzed decellularized bone scaffolds *in vitro* and reported the recellularization of the scaffolds. Recellularization of bone scaffolds have been successfully performed with human mesenchymal stem cells (hMSCs; n = 13), rat mesenchymal stem cells (rMSCs; n = 12), adipose-derived stem/stromal cells (ADSCs; n = 7), mouse MC_3T_3-E_1 cell line (n = 6), NIH/3T3 cell line (n = 4), human umbilical vein endothelial cells (HUVECs; n = 3), periosteum-derived cells (PDCs; n = 2), mouse primary calvarial cells (mPCs; n = 2), human embryonic stem cells-derived mesodermal progenitors (hESCs-MP; n = 2), C2C12 cell line (n = 2), mouse mesenchymal stem cells (mMSCs), rat multipotent adult progenitor cells (rMAPCs), mesenchymal progenitors from human pluripotent stem cells (hPSCs-MP), dental pulp stem cells (DPSCs), amniotic-derived mesenchymal stem cells (af-MSCs), human induced pluripotent stem cells derived mesenchymal progenitor (ipsc-Mp), rat tendon-derived stem cells (rTDSCs), human smooth muscle cells (hSMCs), umbilical cord blood-derived cells (UCBDSCs), bone-marrow derived macrophage (BM-Mø), rabbit osteoblast cells, rabbit fetal osteoblast cells, rat osteoblast cells, human osteoblast cells, human fibroblast cells, and MG-63 cell line (n = 1, each one). While 11 studies have not performed recellularization. Out of these 11 studies, 3 assessed the microstructure and macrostructure of decellularized bone (Bracey et al., 2018; Jeong et al., 2019; Tran et al., 2018), and 8 studies have developed implant approaches to evaluate the surgical suitability of the bone grafts (Anisimova et al., 2015; Borges et al., 2009; Chen et al., 2010; Guo et al., 2020; Huang et al., 2017; Jeong et al., 2016; Lin et al., 2018; You et al., 2018) (Tables 1 and 2).

42 studies evaluated *in vivo* bone regeneration and remodeling of decellularized scaffolds in different animal species such as rat, rabbit, mouse, dog, pig, and chick embryo (Tables 1 and 2).

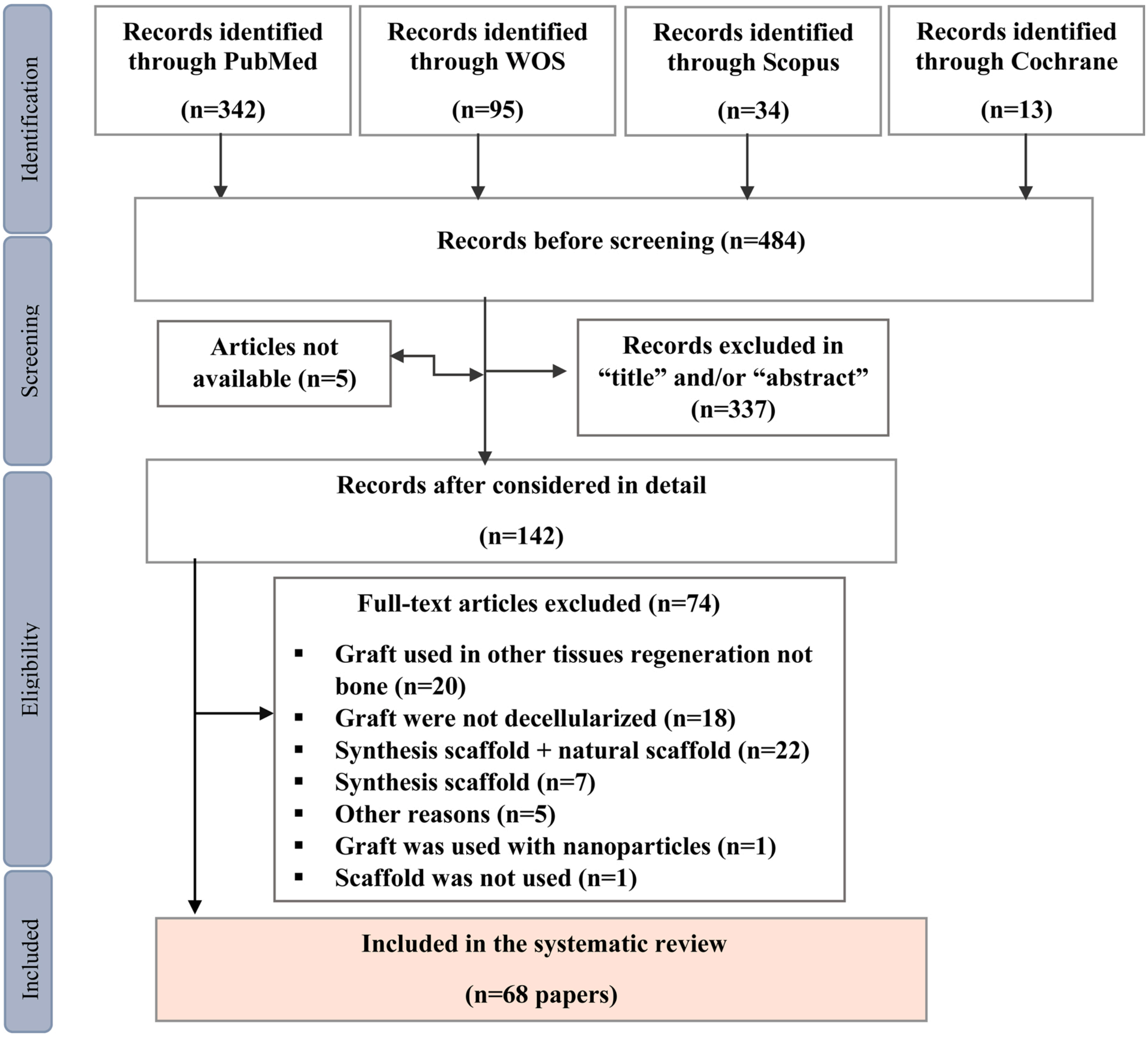

Fig. 1. Flow diagram for study identifuication and selection.

Run-related transcription factor 2 (Runx-2; n = 20), osteocalcin (OCN; n = 18), osteopontin (OPN; n = 14), alkaline phosphatase (ALP; n = 12), collagen type 1 (Col1; n = 8), bone sialoprotein (BSP; n = 8), bone morphogenic protein-2 (BMP-2; n = 4), collagen type1 alpha1 (ColA1; n = 4), alkaline phosphatase liver/bone/kidney (ALPL; n = 4), osterix (OSX; n = 3), osteonectin (ON; n = 2), integrin binding sialoprotein (IBSP; n = 2), platelet-derived growth factor receptor beta (PDGFRB), phosphate-regulating neutral endopeptidase (PHEX), podoplanin, BMP-4 and BMP-7, thanatophoric dysplasia type 1 (TD-1), and matrix metallopeptidase 13 (MMP13) (n = 1, each one) were the most studied genes. In terms of protein expression, osteocalcin (OCN; n = 13), osteopontin (OPN; n = 12), collagen I (col I; n = 8), bone sialoprotein (BSP; n = 5), run-related transcription factor 2 (RUNX2; n = 4), osteonectin (ON; n = 3), alkaline phosphatase (ALP; n = 3), BMP-2, and β-actin (n = 1, each one) were the main parameters. Mineralization capacity was assessed using ALP activity (n = 20), calcium deposits (n = 17) and collagen X depositions (n = 1).

Based on our knowledge, 17 studies out of 68 studies used the human tissue for a generation of the decellularized bone scaffolds. Seven research groups used the decellularization of human bone (Abedin et al., 2018; Ferro et al., 2012; Huang et al., 2017, 2012; Sladkova et al., 2019; Smith et al., 2017, 2015). The other ten researches used the decellularized human placenta vessel selves (DPVs) (Inglis et al., 2019), decellularized human adipose tissue (DAT) (Mohiuddin et al., 2019), human amniotic membrane (HAM) (Fenelon et al., 2020; Li et al., 2015), human teeth (dentin matrix) (Guo et al., 2020), human acellular dermal matrix (ADM) (Borges et al., 2009; Jeong et al., 2016; Kim et al., 2012; Pappalardo and Guarnieri, 2013), and human nail bed tissue (DNB) (Yu et al., 2020) as a scaffold. Other studies used the acellular animal tissues for bone scaffolds, including bovine (n = 21), porcine (n = 17), rat (n = 5), rabbit (n = 3), sheep (n = 3), mouse (n = 1), dog (n = 1), equine (n = 1), and Fish (n = 1). Two studies compared allograft and xenograft tissues (Anisimova et al., 2015; Sladkova et al., 2019). Cancellous bone was the most frequently used tissue (n = 36), followed by periosteum (n = 5), pericardium (n = 3), calvaria bone (n = 2), cartilage (n = 2), Small intestinal submucosa (SIS) (n = 2), skin (n = 2), kidney (n = 1), and scapula bone (n = 1) (Tables 1 and 2).

The pore size of the scaffolds was referred to in 9 studies, ranging from 200−1000 μm (1 mm), while porosity was reported in 3 studies. The biomechanical test was performed in 21 studies with a compression test (n = 11), a tensile test (n = 9), and suture retention strength (n = 1) (Tables 1 and 2).

3.2. *Allograft-derived bone scaffold*

A suitable environment for cellular behaviors like proliferation,

Table 1
Tissues, decellularization techniques, biomechanical test, recellularization methods, and *in vivo* implant of acellular allograft- derived bone scaffold.

Nr	Author (s)	Tissues	Decellularization methods	*In vitro* recellularization	*In vivo* implant	Biomechanical test	Pore size
1	Abedin et al. (2018)	Human femoral head	Freezing/thawing 6 cycles; 0.25 % trypsin; 2.5 % SDS.	The scaffolds were seeded with rABMC.	NA	NA	NA
2	Anisimova et al. (2015)	Mouse cancellous bone	4% sodium chlorite in dH_2O for 1−4 months; 0.9% NaCl; dimethyl; 0.9% NaCl; dimethyl larizationsulf oxide and 6% aseptic dextran.	NA	Heterotopic transplantation: DECM from mouse's femur bone were implanted under the dorsal skin of mice.	Compression test	NA
3	Chen et al. (2015)	Rabbit periosteum	Freeze-thaw for 3 cycles; 2% Triton x-100; 1% SDS; 100 U/mL DNase under shaking.	PDCs were seeded on D-periosteum.	D-periosteum were implanted subcutaneously into the backs of rabbit.	Tensile test	NA
4	Chen et al. (2010)	Porcine rib	5 mM NaN_3; 0.2 N NaOH and 1.5% Triton X-100; methanol/chloroform (1:4) twice; ethanol; 0.1 N NaOH and 1% Triton X-100; methanol/chloroform (1:4); 30% H_2O_2 twice; ethanol; methanol/chloroform (1:1); ethanol 3 times; distilled water 3 times.	NA	ACBM with the ADSC transfected by rhBMP-2 and rhVEGF were implanted in minipigs with ulna bone defect.	NA	NA
5	Elkhateb et al. (2018)	Rat dermis of the skin	Freezing-thawing for three cycles; soaking with zwitterion eluent in the ultrasonic cleaning machine; distilled water.	BM-MSCs were seeded in the ADM scaffold.	ADM with and without BM-MSCs were implanted into the rat with critical size defect.	NA	NA
Nr	Author (s)	Tissues	Decellularization methods	*In vitro* recellularization	*In vivo* implant	Biomechanical test	Pore size
7	Lee et al. (2014)	Rat calvaria bone matrix	0.5 % SDS and 0.1 % NH_4OH under shaking.	MC_3T_3-E_1 were seeded on DECBM	DECBM seeded with rat MAPCs and implanted into rat calvaria with critical size defect.	Compression test	NA
8	Lee et al. (2016)	Rat calvaria bone	0.5 % SDS and 0.1 % NH_4OH; dH_2O for 3 weeks.	rMSCs were seeded on DECBM.	rMSCs with DECBM were implanted into rat calvaria with critical size defect.	NA	NA
9	Lin et al. (2018)	Rabbit periosteum	Freezing-thawing; 1% Triton x-100 in dH_2O under shaking; 1% SDS in dH_2O; 200 U/mL DNase.	NA	D-periosteum ECM implanted into rabbit with critical bone defect.	NA	NA
10	Pennington et al. (2015)	Rabbit tibiofibulas bone	PBS with 0.1 % EDTA; 10 mM Tris and 0.1 % EDTA; 10 mM Tris and 0.5 % SDS; 50 U/mL DNase and 1 U/mL RNase and 10 mM Tris.	af-MSCs were seeded on scaffolds.	Scaffold with cell were implanted into rabbit with critical size tibiofibular defect.	Compression teste	NA
11	Sladkova et al. (2019)	Human femoral head	0.1 % EDTA in 10 mM Tris; 0.5 % SDS in 10 mM Tris; 100 U/mL DNase/RNase in 10 mM Tris.	The scaffolds were seeded with iPSCs and transferred to bioreactors.	NA	NA	NA
12	Smith et al. (2015)	Human femoral head	dH_2O preheated to 60 °C under Shaking; followed by centrifugating at room; sonicated on sterilant solution at 60 °C; 70% ethanol.	MSCs were seeded on decellularized bone.	NA	Compression teste	NA
13	Smith et al. (2017)	Human femoral head	dH_2O preheated to 60 °C under Shaking; followed by centrifugating at room; sonicated on sterilant solution at 60 °C; 70% ethanol.	BM-MSCs were seeded on a decellularized bone.	NA	NA	NA

NA: not available, MSC: mesenchymal stem cell, BM-MSC: bone marrow-mesenchymal stem cell, iPSC: human induced pluripotent stem cells derived mesenchymal progenitor, rABMC: rat adherent bone marrow cell, Pe-MSC: periosteum mesenchymal stem cell, SDS: sodium dodecyl sulfate, dH_2O: deionized water, NH_4OH: ammonium hydroxide, PBS: phosphate buffer saline, af- MSC: amniotic derived mesenchymal stem cell, EDTA: Ethylenediamine tetraacetic acid, rMSC: rat mesenchymal stem cell, PDC: periosteum-derived cell, DECBM: decellularized bone matrix, MAPC: multipotent adult progenitor cell, D-periosteum: decellularized-periosteum, ACBM: acellular bone matrix, ADSC: adipose-derived stem cell, NaOH: Sodium hydroxide, NaN_3: Sodium azide, rhBMP-2: recombinant human bone morphogenetic protein-2, rhVEGF: recombinant human vascular endothelial growth factor, ADM: acellular dermal matrix.

differentiation, and migration can be provided by scaffolds (Tabata, 2009). Among all-natural and synthetic scaffolds, decellularized allografts (mostly human femoral head bones) show several advantages including minimized immune response, retaining biological activities due to their structural characterization similar to native tissues, and supporting recellularization (Ebraheim et al., 2001; Varettas and Taylor, 2011). According to Smith's et al. (2015) study, which has designed a decellularization method based on wash-centrifuge phases (dH_2O preheated to 60 °C under shaking, followed by centrifuging at room temperature) and sonication (sterilant solution containing 3% v/v hydrogen peroxide and 0.02 % v/v peroxy_acetic acid at 60 °C than in 70 % v/v ethanol at 21 °C), the protocol could remove the marrow elements of human bone. This scaffold without need osteogenic medium promoted the differentiation of MSCs to osteogenic lineage, and thus, indicated that the ECM proteins and growth factors remain functional (Smith et al., 2015). After two years, Smith et al. (2017) used the same methods (washed bone) to investigate the impacts of donor age. In this study, decellularized human bones from young and old donors were seeded by MSCs from young and old donors. It demonstrated that the ability of the bone of old donors to support osteogenic differentiation is better than the bone of young donors. In contrast, the differentiation capacity of MSCs from young donors was better than the old donor (Smith et al., 2017). Recently, Sladkova et al. (2019) designed a protocol that was used for the preparation of a decellularized bone scaffold from cadaveric human bone. This protocol used of (0.1 % EDTA in 10 mM Tris at 4 °C, 0.5 % SDS in 10 mM Tris and 100 U/mL DNase/RNase in 10 mM Tris at 37 °C) to remove cellular elements from bone. The scaffold was combined with human iPSC-MP cells and osteogenic medium and then transferred to perfusion bioreactor. Results showed that the scaffold supports osteogenic differentiation and mineralization (Sladkova et al., 2019). MSCs of periosteum developed a complex matrix and an osteoblastic phenotype on the acellular bone scaffold (Ferro et al., 2012). We have shown that demineralized and decellularized human epiphyseal bone scaffold able to induce osteoblast differentiation and mineralization without the need for osteogenic factors (Abedin et al., 2018). *In vivo* or *in vitro* studies that used animal tissues as a scaffold, have shown high

Table 2
Tissues, decellularization techniques, biomechanical test, recellularization methods, and *in vivo* implant of acellular xenograft- derived bone scaffold.

Nr	Author (s)	Tissues	Decellularization methods	*In vitro* recellularization	*In vivo* implant	Biomechanical test	Pore size
1	Alom et al. (2018)	Bovine cancellous bone	dH_2O with 0.05% trypsin and 0.02% ethylenediaminetera acetic acid for 24 h.	mPCs and C_2C_{12} cell line were seeded on scaffold.	NA	NA	NA
2	Anisimova et al. (2015)	Dog trabecular bone	4% sodium chlorite in dH_2O for 1−4 months; 0.9% NaCl; dimethyl; 0.9% NaCl; dimethyl larizationsulf oxide and 6% aseptic dextran.	NA	Orthotopic xenogenic transplantation: DECM from dog's fibula were implanted in an artificial defect of the rat tibia.	Compression test	NA
3	Arca et al. (2011)	Porcine cancellous bone	NA	hMSCs were seeded onto the DBM scaffold.	NA	NA	NA
4	Bagher et al. (2012)	Sheep trabecular bone	Freezing/thawing: liquid nitrogen freezing −20 °C; isotonic salin; gulactosidase.	Rabbit osteoblast cells were seeded into scaffold.	Scaffolds were implanted into a rabbit with tibia defect.	NA	NA
5	Bai et al. (2014)	Bovine pericardium	0.25 % Triton x-100 and 1% sodium deoxy cholate under shaking; 200 mg/mL DNase and RNase 150 mg/mL.	NIH/3T3 cells were seeded into decellularized BP.	Acellular BP was implanted in a rabbit with mandibular defects.	Tensile test	NA
6	Bernhard et al. (2017)	Bovine cancellous bone	PBS with 0.1 % EDTA; 10 mM Tris and 0.1 % EDTA; 10 mM Tris and 0.5 % SDS under shaking; 100 U/mL DNase and 1 U/mL RNase with 10 mM Tris.	hASCs were seeded into the decellularized bone scaffold.	Cell seeded scaffolds were implanted into critical-size defects in the femur of rat.	NA	NA
Nr	Author (s)	Tissues	Decellularization methods	*In vitro* recellularization	*In vivo* implant	Biomechanical test	Pore size
7	Borges et al. (2009)	Human ADM	NA	NA	ADM were implanted in dog with mandibular pre-molars defect.	NA	NA
8	Bracey et al. (2018)	Porcine cancellous bone	dH_2O; 0.05% trypsin-EDTA; DMEM with antimicrobial 100 U/mL penicillin, 100 µg/mL streptomycin, 0.25 µg/mL amphotericin B; 1000 ml DNase/ RNase-free; 1.5% peracetic acid and 2% Triton X-100 in ddH_2O under shaking.	NA	NA	Compression test	474.2 µm
9	Bracey et al. (2019a)	Porcine cancellous bone	dH_2O; 0.05% trypsin-EDTA; DMEM with antimicrobial 100 U/mL penicillin, 100 µg/mL streptomycin, 0.25 µg/mL amphotericin B; 1000 ml DNase/ RNase-free; 1.5% peracetic acid and 2% Triton X-100 in ddH_2O under shaking.	C_2C_{12} and MC_3T_3-E1 were seeded on scaffold.	The scaffolds were preseeded with MC_3T_3-E1 and were implanted in right Flank of C_{57}BL/6.	NA	NA
10	Bracey et al. (2019b)	Porcine cancellous bone	dH_2O; 0.05% trypsin-EDTA; DMEM with antimicrobial 100 U/mL penicillin, 100 µg/mL streptomycin, 0.25 µg/mL amphotericin B; 1000 ml DNase/ RNase-free; 1.5% peracetic acid and 2% Triton X-100 in ddH_2O under shaking.	Murine 3T3 cell monolayers	NA	NA	NA
11	Burgkart et al. (2014)	Rat kidney	SDS concentrations of 0.25 %, 0.5 %, 0.66 %, and 1% for 0.5, 1.2 and 4 h; for second part the concentration of SDS was 0.66% for l h; dH_2O; SDS for 30 min.	First part: Primary human osteoblasts were seeded into the decellularized kidneys. Second part: Primary human osteoblasts and HUVEC were co-cultured within bioscaffold.	NA	NA	NA
12	Butorina et al. (2020)	Porcine SIS	NA	Rat BM-MSCs were seeded in scaffold.	NA	NA	NA
Nr	Author (s)	Tissues	Decellularization methods	*In vitro* recellularization	*In vivo* implant	Biomechanical test	Pore size
13	Cunniffe et al. (2015)	Hypertrophiccartilage tissue	Freezing/thawing; 0.1 % SDS; 10 U/mL DNase and 10 U/mL RNase.	hMSCs were seeded into the HT scaffolds.	Scaffolds were implanted in rat with femoral defects.	NA	NA
14	De Peppo et al. (2013)	Bovine trabecular bone	PBS with 0.1 % EDTA; PBS with 0.1 % EDTA; 10 mM Tris and 0.1 % EDTA under shaking; 0.5 % SDS and Tris 10 mM under shaking; DNase/RNase in 10 mM Tris.	Scaffold seeded with hPSC-MPs were cultivated in perfusion bioreactor.	hPSC-MPs engineered bone constructs were implanted in mice.	NA	NA
15	Emami et al. (2020)	Bovine Scapula bone	PBS with 0.02 % EDTA and 0.05 % trypsin; distilled water; 1% Triton X-100 under shaking. PBS with either 0.5 and 1% SDS; 1% Triton X-100 under shaking. 0.5 % SLES with PBS and 1% Triton X-100.	MG-63 cell line were seeded on each decellularized scaffold.	NA	NA	NA
16	Fénelon et al. (2020)	Human amniotic membrane	Trypsin/EDTA, 0.125 %; transferring in a solution composed of 8 mM CHAPS, 25 mM EDTA, 0.12 mM NaOH and 1 M NaCl under agitation.	hBMSCs were seeded in DL-HAM scaffold.	DL-HAM scaffold were implanted onto mice with femoral defect.	Suture retention strength	NA
17		Bovine trabecular bone			NA	NA	NA

(*continued on next page*)

Table 2 (*continued*)

Nr	Author (s)	Tissues	Decellularization methods	*In vitro* recellularization	*In vivo* implant	Biomechanical test	Pore size
	Frohlich et al. (2010)		PBS with 0.1 % EDTA; 10 mM Tris and 0.1 % EDTA; 10 mM Tris and 0.5 % SDS; 50 U/mL DNase and 1 U/mL RNase and 10 mM Tris.	hASCs were seeded onto the scaffold in perfusion bioreactor.			
18	Gardine et al. (2015)	Bovine cancellous bone	Freezing/thawing; 1% Triton X-100 8 h; 0.1 % Triton X-100 16 h under shaking.	hASCs were seeded into the scaffold.	The scaffold were implanted in a maxillary sinus augmentstion model in sheep.	NA	NA
Nr	Author (s)	Tissues	Decellularization methods	*In vitro* recellularization	*In vivo* implant	Biomechanical test	Pore size
19	Gardine et al. (2015)	Bovine pericardium	Freezing/thawing 2 cycles; 0.1 % SDS and 0.1 % EDTA under shaking; 50 U/mL DNase and 1 U/mL RNase in PBS containing 10 mM magnesium chloride and BSA.	Human fibroblast cells were seeded on the scaffold.	Decellularized pericardium scaffolds were implanted in the abdominal area of rats.	NA	NA
20	Gawlitta et al. (2015)	Equine cartilage	Freezing/thawing; 0.25 % trypsin-EDTA; 50 U/mL DNase and 1 U/mL RNase in 10 mM Tris-HCL under agitation; 10 mM Tris-HCL; 1% V/V Triton X-100 in PBS.	hMSCs were seeded onto the CDM scaffolds.	MSCs seeded CDM scaffolds were implanted into the athymic nude rats.	NA	NA
21	Grayson et al. (2008)	Bovine trabecular bone	PBS with 0.1 % EDTA; 10 mM Tris and 0.1 % EDTA; 10 mM Tris and 0.5 % SDS; 50 U/mL DNase and 1 U/mL RNase and 10 mM Tris.	hMSCs were seeded into the scaffold.	Decellularized bone scaffolds were implanted subcutaneously into the ventral regions of rats.	NA	NA
22	Guo et al. (2020)	Human teeth	Decalcified: 0.5 mol/l HCL; centrifuge at 1000 rev/min. Decellularized: (hypotononic NaCl); trypsin and EDTEA; Triton X-100.	NA	Scaffold was implanted in rat with cranio-parietal bone-defect.	NA	NA
23	He et al. (2020a)	Sheep periosteum	Freeze-thaw 3 times; 1% (v/v) Tritonx-100; 0.2 % (wt/v) SDS under shaking; DNase (100 U/mL) and RNase (75 μg/mL).	Mouse MC_3T_3-E1 was seeded on scaffold.	AP was implanted in the rabbit with cranial defects.	Tensile test	NA
24	He et al. (2020b)	Sheep periosteum	Freeze-thaw 3 times; 1% (v/v) Tritonx-100; 0.2 % (wt/v) SDS under shaking; DNase (100 U/mL) and RNase (75 μg/mL).	Mouse MC_3T_3-E1 was seeded on scaffold.	AP was implanted into the back of rat.	NA	NA
25	Huang et al. (2012)	Human cancellous bone	NA	rBM-MSCs were seeded into the ACBM.	ACBMs without cell were implanted into the bilateral ectogluteus of rats.	NA	75−600 μm
26	Huang et al. (2017)	Human femoral head	NA	NA	DBM scaffolds were implanted in the periosteal flap in rabbit.	Compression teste	200−400 μm
Nr	Author (s)	Tissues	Decellularization methods	*In vitro* recellularization	*In vivo* implant	Biomechanical test	Pore size
27	Inglis et al. (2019)	Human placenta vessel sleeve	PBS with heparin 50 IU/mL and penicillin/ streptomycin; freezing and thawing; perfusion with a hypertonic (1.2 % NaCl) and hypotonic (0.4 % NaCl); 1% Triton X-100 and 0.02 % w/w EDTA; DNase (200 IU); 0.1 % w/v PAA.	Decellularized PVS was recellularized with HUVEC cells.	Chick with defect femur (embryonic 18 day)	NA	NA
28	Jeong et al. (2016)	Human acellular dermal matrix	NA	NA	PRP with ADM were implanted into rabbit with calvarial defects.	NA	NA
29	Jeong et al. (2019)	Rat cancellous bone	0.5 % SDS and 0.1 % NH_4OH in PBS.	NA	NA	NA	1 μm^2
30	Kaempfen et al. (2015)	Bovine cancellous bone	NA	rBMSCs were seeded into the DBM scaffold.	DBM with fibrin hydrogel were implanted in rabbit with orthotopic segmental defect.	NA	NA
31	kedong et al. (2014)	Porcine cancellous bone	3 mM NaN3 at 4 °C; 1.1 chloroform/methanol; double dH_2O 3 times; 3% Triton X-100 + 7% sodium deoxycholate; 20% H_2O_2.	hADSCs were combined with scaffold and cultured in spineer flask.	NA	Tensile test	284.5μm
32	Kim et al. (2012)	Human dermal tissue	NA	ASCs were seeded into the ADM scaffold.	ADM with and without ASCs were implanted into the athymic nude rats.	NA	NA
33	Lau et al. (2019)	Tilapia skin	2.5 U/mL dispase; 1% SDS; 25 U/mL nuclease; 1% SDS.	$MC_3T_3.E_1$ cells were seeded onto the scaffold.	The scaffolds were implanted in rat with calvarial defect.	Tensile test	NA
34	Lee et al. (2020)	Bovine cancellous bone	Demineralized then 0.6 N citric acid and distilled water.	Rat osteoblasts were seeded in bdECM scaffold.	bdECM scaffold were implanted into mouse with calvarial defects.	NA	NA
35	Leng et al. (2020)	Porcine cancellous bone	Methanol and chloroform 1:1; processing with an ultrasonic cell crusher for 3 cycles; PBS and ddH_2O; 0.5% dipase and 1% Triton X-100 in 0.05 M/l^- Tris-HCL under shaking for 3 times; PBS and ddH_2O; freez-deried.	BMSCs were seeded in the decellularized DBM scaffold and PRP loaded DBM scaffold.	The scaffolds was implanted into rabbit with critical size defect.	Compression test	NA
36	Li et al. (2017)	Porcine SIS	NA			NA	NA

(*continued on next page*)

Table 2 (*continued*)

Nr	Author (s)	Tissues	Decellularization methods	*In vitro* recellularization	*In vivo* implant	Biomechanical test	Pore size
				NIH/3T3, $MC_3T_3.E_1$ and BMSC cells were seeded on SIS scaffold.	The SIS scaffold was implanted in mouse with calvaria defect model.		
37	Li et al. (2015)	Human amniotic membrane	1% Triton X-100 (200 ml); distilled water (200 ml) and 0.1% SDS (200 ml) under shaking.	rBM-MSCs were seeded into the AHAM scaffold.	Multilayered AHAM were implanted into rat with tibia defect.	Tensile test	NA
38	Liu et al. (2018)	Porcine cancellous bone	2% SDS, 10 mM Tris; methanol chloroform, ethanol and 0.25 % trypsin; ddH_2O; 50 U/mL DNase, 1 U/mL RNase, 10 mM Tris, ddH_2O.	hSMCs and HUVECs were co-cultured within the DB scaffold, fibrin hydrogel was added and then were cultured in the bioreactor.	NA	NA	NA
39	Marcos et al. (2012)	Bovine trabecular bone	PBS with 0.1 % EDTA; 10 mM Tris and 0.1 % EDTA under shaking; 0.5 % SDS and Tris 10 mM for 24 h.	hESCs-MP were seeded into the bone scaffold.	NA	Compression test	4μm-1 mm
40	Marolt et al. (2012)	Bovine trabecular bone	PBS with 0.1 % EDTA; 10 mM Tris and 0.1 % EDTA; 10 mM Tris and 0.5 % SDS; 50 U/mL DNase and 1 U/mL RNase and 10 mM Tris.	Scaffold seeded with hESC-MPs were cultivated in perfusion bioreactor.	hESC-MPs engineered bone constructs were implanted in immuodeficient mice.	NA	NA
Nr	Author (s)	Tissues	Decellularization methods	*In vitro* recellularization	*In vivo* implant	Biomechanical test	Pore size
41	Mohiuddin et al. (2019)	Human adipose tissue	Freezing / thawing 3 times; dH_2O; 0.5 M and 1 M sodium chloride; dH_2O; 0.25% trypsin; isopropanol; dH_2O; 1% Triton x-100 and dH_2O.	Both ASC and OIASC cells were suspended in DAT hydrogel scaffold.	The scaffolds were implanted in C57BL/6 mice with Femoral defect.	NA	NA
42	Nakamura et al. (2019)	Porcine cancellous bone	SDS treatment: 10 % iodine; 10 mM Tris buffer containing 0.1 % EDTA; 0.5 % agar and 1.25 % EDTA; 10 mM Tris and 0.1 % EDTA and 0.1 % SDS; 50 mM Tris-HCL and 10 mM magnesium chloride; 50 μg/mL bovine serum albumin; 50 U/mL DNase and 1 U/mL RNase; 0.1 % EDTA in PBS under shaking. HHP treatment: Pressurizing at 980 MPa and 10 °C; 50 mM magnesium chloride; 0.2 mg/mL DNase I; 80 % ethanol under shaking.	hMSCs were seeded on DCB scaffold.	HHP and SDS DCBs seeded with hMSCs were implanted subcutaneously in mice.	NA	NA
43	Nakamura et al. (2020)	Porcine cancellous bone	Pressurizing at 980 MPa and 10 °C; 50 mM magnesium chloride; 0.2 mg/mL DNase I; 80 % ethanol under shaking.	hMSCs: rMSCs were seeded in DCBs. rBMCs were seeded in DCBs.	NA	NA	NA
44	Nie et al. (2020)	Porcine cancellous bone	PBS with 1% Triton X-100 and 0.5 % sodium deoxycholate; DNase I (150 U/mL) and RNase (100 μg/mL); 100 % ethanol.	hMSCS were seeded into DBM scaffold.	NA	Compression test	500 μm
45	Paduano et al. (2017)	Bovine cancellous bone	0.5 M HCL; chloroform/methanol; 0.05 % trypsin; 0.02 % EDTA; 1 mg/mL pepsin in 0.01 M HCL.	DPSCs were seeded onto decellularized bECM hydrogels.	NA	NA	NA
46	Pappalardo et al. (2013)	Human acellular dermal matrix	NA	MSCs were seeded into ADM	NA	NA	NA
Nr	Author (s)	Nr	Decellularization methods	*In vitro* recellularization	*In vivo* implant	Biomechanical test	Pore size
47	Qing et al. (2019)	Bovine cancellous bone	Hydrochloric acid 0.5 N; methanol:ethanol 1:1; 1% Triton X-100 and sodium deoxycholate 0.5 %; 150 IU/mL DNase and 100 μg/mL RNase.	rBMSC, rTDSC cells, and NIH-3T3 fibroblasts were seeded into HPTBM.	The scaffolds were implanted subcutaneously in the dorsal regain of rat.	Tensile test	NA
48	Qiu et al. (2019)	Porcine periosteum	Freezing / thawing 3 times; 1% Triton x-100; 1% SDS; 200 U/mL DNase.	MSCs were seeded in PEM hydrogel.	PEM hydrogel was implanted into the rat with critical- size calvarial defect.	NA	NA
49	Quan et al. (2010)	Porcine cancellous bone	Tris-NaCL for 6 h; 0.6 M HCL; acetone or chloroform/methanol.	UCBDSs were seeded into the scaffold.	NA	NA	250–1000 μm
50	Rashmi et al. (2017)	Bovine cancellous bone	Freeze-thaw for 5 cycles each cycle (liquid nitrogen; hot water at 56 °C, 3% H_2O_2; 70% ethanol).	The rabbit fetal osteoblast cell were seeded on the scaffold.	NA	NA	200–500 μm
51	Sahabipour et al. (2013)	Bovine cancellous bone	Freezing/thawing: 2.5 %, 5% and 8% SDS (w/v) for 8, 3 or 1 h; 75 % ethanol and PBS at room temperature.	Rat MSCs were seeded into the scaffold.	NA	Tensile test	NA
52	Sawkins et al. (2013)	Bovine tibia bone	0.05 % trypsin and 0.02 % ethylenediamine tetraacetic acid under agitation.	mPCs wrere seeded into the dECM hydrogel.	NA	Compression test	NA
53	Sladkova et al. (2019)	Bovine trabecular bone	0.1 % EDTA in 10 mM Tris; 0.5 % SDS in 10 mM Tris; 100 U/mL DNase/RNase in 10 mM Tris.	The scaffolds were seeded with iPSCs and transferred to bioreactors.	NA	NA	NA
54	Tran et al. (2019)	Bovine cancellous bone	Washing with PBS; immersing EtOH under shaking; thermal shock for 4 cycles; 1% Triton X-100; 0.1 % Triton X-100.	NA	NA	NA	NA
Nr	Author (s)	Tissues	Decellularization methods	*In vitro* recellularization	*In vivo* implant		Pore size

(*continued on next page*)

Table 2 (*continued*)

Nr	Author (s)	Tissues	Decellularization methods	*In vitro* recellularization	*In vivo* implant	Biomechanical test	Pore size
						Biomechanical test	
55	You et al. (2018)	Bovine trabecular bone	PBS with 0.1 % EGTA (wt/vol); 10 mM Tris and 0.1 % Triton X-100 (wt/vol); the samples were treated by SC-CO_2.	NA	DBB scaffolds were implanted into the abdominal cavity of mice.	NA	NA
56	You et al. (2020)	Porcine pericardium	NA	hBMSCs and hGFs were seeded on the APP scaffold.	APP was implanted in mouse with critical size-calvarial defect.	Tensile test	NA
57	Yu et al. (2020)	Human nail bed	Heparin 50 U/mL in PBS; Triton X-100 (0.1 %), dH_2O and SDS 0.1% (V/V); penecilin (100 U/mL) and streptomycin (100 mg/mL).	BM-Mø were cultured with the dNB scaffolds and then BMSCs were co-culture with dNB and BM-Mø.	The scaffold was implanted into rat with critical size defect.	NA	NA
58	Zheng et al. (2018)	Porcine cancellous bone	PBS with 0.1 % EDTA; 10 mM Tris, 0.1 % EDTA (wt/vol); 10 mM Tris, 0.5 % SDS (wt/vol); 50 U/mL DNase, 1 U RNase, 10 mM Tris.	BMSCs were seeded on the scaffold.	DBM scaffolds were loaded with IL-4 and were implanted in rat with cranial bone defect.	NA	NA

NA: not available, ADSC: adipose stem cell, SDS: sodium dodecyl sulfate, dH_2O: deionized water, ddH_2O: deionized-distilled water, H_2O_2: hydrogen peroxide, hESC-MP: mesodermal progenitor from human embryonic stem cell, mPC: mouse primary calvarial cell, DPSC: dental pulp stem cell, ipsc-Mp: human induced pluripotent stem cell derived mesenchymal progenitor, HUVEC: human umbilical vein endothelial cell, PBS: phosphate buffer saline, PRP: platelet-rich plasma, ADM: acellular dermal matrix, EDTA: Ethylenediamine tetraacetic acid, SIS: Small Intestinal Submucosa, hASC: human adipose stem cell, rBMSC: rat bone marrow mesenchymal stem cell, rTDSC: rat tendon-derived stem cell, HPTBM: H_2O_2-treated DCDBM, DCDBM: decellularized and demineralized bone matrix, HT: hypertrophic cartilage, CDM: cartilage derived-matrix, DBM: decellularized bone matrix, BSA: bovine serum albumin, HCL: hydro chloric acid, BM-Mø: bone-marrow derived macrophage, dNB: decellularized nail bed, hSMC: human smooth muscle cell, ASC: adipose-derived stem/stromal cell, OIASC: osteo-induced ASC, DAT: decellularized adipose tissue, PDC: periosteum-derived cell, AP: acellular periosteum, IL-4: interleukin-4, DB: decellularized bone, bECM: bone extracellular matrix, BP: bovine pericardium, PVS: placenta vessel sleeve, SLES: sodium lauryl ether sulfate, DL-HAM: decellularized and lyophilized human amniotic membrane, hBMSC: human bone marrow mesenchymal stem cell, NaOH: sodium hydroxide, NaCL: Sodium chloride, CHAPS: 3-[(3-Cholamidopropyl)dimethylammonio]-1-propanesulfonate, hMSC; human mesenchymal stem cell, ADM: acellular dermal matrix, bdECM: bone decellularized ECM, AHAM: acellular human amniotic membrane, SC-CO_2: supercritical carbone dioxide, DBB: decellularized bovine bone, EGTA: ethylene glycol tetraacetic acid, HHP: high hydrostatic pressure, UCBDC: umbilical cord blood-derived cell, hGF: human gingival fibroblast, APP: acellular porcine pericardium, hPSC-MP: mesenchymal progenitor from human pluripotent stem cell, rBMC: rat bone marrow cell, EtOH: ethanol alcohol, PEM: periosteal extracellular matrix.

biocompatibility of seeded decellularized scaffolds, enhancement the osteogenic differentiation and mineralization (Anisimova et al., 2015; Chen et al., 2015, 2010; Elkhateb et al., 2018; Lee et al., 2016, 2014; Lin et al., 2018; Pennington et al., 2015) (Tables 1–4). Several authors performed subcutaneous tissue decellularization according to combined protocols that used an enzymatic method and chemical method and mechanical method (Abedin et al., 2018; Chen et al., 2015; Lin et al., 2018), the enzymatic method and the chemical method was performed by three authors (Elkhateb et al., 2018; Pennington et al., 2015; Sladkova et al., 2019), the chemical method and mechanical method (Lee et al., 2014; Smith et al., 2017, 2015), the chemical method alone (Anisimova et al., 2015; Chen et al., 2010; Lee et al., 2016), and one study has used commercially decellularized bone scaffold from the tissue bank (Ferro et al., 2012). Eight studies used animal bone tissues as an allograft. The decellularized animal tissues that used as the allograft scaffold for the generation of the bone are rabbit periosteum (Chen et al., 2015; Lin et al., 2018), rabbit tibia bone (Pennington et al., 2015), rat calvaria (Lee et al., 2016, 2014), mouse cancellous bone (Anisimova et al., 2015), rat skin (Elkhateb et al., 2018), and porcine rib (Chen et al., 2010).

3.3. Xenograft bone scaffold

Xenogenic ECM scaffolds can be generated from different decellularized tissues. This study aimed to define the function of the decellularized xenograft tissues in bone repair and remodeling. 12 studies used human tissues as xenograft and 45 others used animal tissues as a bone scaffold. A functional bone graft was regenerated by using a human pedicle periosteal flap as an *in vivo* bioreactor and a DBM (decellularized femoral head bone) as a bio-scaffold in a rabbit model (Huang et al., 2017). On the other hand, Huang et al. (2012) reported that the human acellular cancellous bone matrix has poor osteoinductivity, but it could mimic the microenvironment of bone marrow and acted as a stem cell niche for tissue engineering (Huang et al., 2012). Inglis et al. (2019) used the DPVs as a periosteal protective sleeve to enhance bone regeneration in embryonic day 18 chick femurs. Decellularization was performed with (PBS with heparin 50 IU/mL and 1% penicillin/streptomycin; freeze and thaw technique; perfusion with a hypertonic (1.2 % NaCl) and hypotonic (0.4 % NaCl); 1% Triton x-100 and 0.02 % w/w EDTA; DNase (200 IU); 0.1 % w/v PAA). DPVs were recellularized with HUVECs and cultured on the chorioallantoic chick membrane. Excellent cell viability of allogeneic cells (HUVECs) seeded onto DPVs and biocompatibility (100 % survival) and integration (70 %) of the DPVs, as well as higher levels of bone formation and visible blood vessel, indicated the potential of decellularized grafts to augment bone healing (Inglis et al., 2019). Mohiuddin OA et al. (2019) showed a novel application of decellularized adipose tissue (Frozen/thawed 3 times; dH_2O for 48 h; 0.5 M and 1 M sodium chloride; dH_2O overnight; 0.25 % trypsin; isopropanol; dH_2O overnight; 1% Triton x-100 and dH_2O) as a bioscaffold in combination with ASCs for the regeneration of cortical-sized long bone defects (Mohiuddin et al., 2019). Guo K et al. (2020) used human tooth as a scaffold and Yu Y et al. (2020) used human nail bed tissue with BM-Mø (bone marrow-derived macrophage) that the cells were indirectly cultured with the scaffold. The scaffold modulated macrophage polarization into M2, thus promoted the osteogenesis and bone regeneration of bone marrow mesenchymal stem cells (BMSCs) *in vitro* and *in vivo* (Guo et al., 2020; Yu et al., 2020). Four studies used ADM (composed of human dermis ECM) that undergoes a multi-step proprietary process to removes cellular components that can lead to tissue rejection. ADM consists of collagens, especially collagen type one, glycosaminoglycans, elastins and proteins that support vascularization, cell proliferation, and tissue remodeling and is similar to the ECM of bone (Cummings et al., 2005). *In vitro* results indicated one of the most important biological features of an ADM seems to be the ability to permit stem cell adhesion. This adhesion is important because the cells create bridges that permit them to interact with neighboring

Table 3
In vitro outcomes.

Nr	Author (s)	Osteogenic differentiation	Mineralization	New bone formation
1	Alom et al. (2018)	Y	Y	NA
2	Arca et al. (2011)	Y	Y	NA
3	Bagher et al. (2012)	NA	Y	NA
4	Bernhard et al. (2017)	Y	NA	Y
5	Bracey et al. (2019a)	NA	Y	NA
6	Burgkart et al. (2014)	Y	Y	NA
7	Butorina et al. (2020)	NA	Y	NA
8	Cunniffe et al. (2015)	NA	Y	NA
9	De Peppo et al. (2013)	Y	Y	Y
10	Fenelon et al. (2020)	NA	Y	NA
11	Fröhlich et al. (2010)	NA	Y	NA
12	Gardin et al. (2015)	Y	NA	NA
13	Grayson et al. (2008)	Y	Y	NA
14	He et al. (2020b)	Y	Y	NA
15	Huang et al. (2012)	Y	NA	NA
16	Kedong et al. (2014)	Y	Y	NA
17	Lau et al. (2019)	Y	Y	NA
18	Lee et al. (2020)	Y	Y	NA
19	Li et al. (2017)	Y	Y	NA
20	Li et al. (2015)	Y	Y	NA
21	Marcos-Campos et al. (2012)	Y	Y	Y
22	Marolt et al. (2012)	Y	Y	Y
23	Nakamura et al. (2019)	Y	Y	NA
24	Nie et al. (2020)	Y	Y	NA
25	Paduano et al. (2017)	Y	Y	NA
26	Pappalardo et al. (2013)	NA	Y	NA
27	Qing et al. (2019)	Y	NA	NA
28	Qiu et al. (2020)	Y	Y	NA
29	Sladkova et al. (2019)	Y	Y	Y
30	You et al. (2020)	Y	Y	NA
31	Yu et al. (2020)	Y	Y	NA
32	Zheng et al. (2018)	Y	Y	NA

Y: available, NA: not available.

cells. *In vivo* results showed that ADM successfully integrates with the host tissue, and cells/ADM implants promote new bone formation more rapidly than ADM alone (Borges et al., 2009; Jeong et al., 2016; Kim et al., 2012; Pappalardo and Guarnieri, 2013). Based on our knowledge, two studies have investigated the potential of decellularized human amniotic membrane (DL-HAM) for bone healing. They designed a decellularization protocol that did not damage the integrity of the basement membrane components, which is essential to promote cell seeding. They have shown the ability of DL-HAM to promote BMSCs osteo-differentiation *in vitro*. *In vivo*, DL-HAM enhanced bone formation (Fenelon et al., 2020; Li et al., 2015).

The composition of the native tissues can be changed with different decellularization protocols. Non-ionic detergents, ionic detergents, and various enzymes are several chemicals used to remove cell components, which have been introduced as decellularizing agents (Lumpkins et al., 2008).

The protocols for xenograft tissue decellularization were analyzed in this systematic review, consisting of a combination of mechanical, chemical, and enzymatic treatments that extract cells and preserve the structural ECM components (Table 2). Several authors performed subcutaneous tissue decellularization according to combined the mechanical disruption of the tissue (i.e. freezing-thawing or agitation) and enzyme digestion (i.e. by DNase, RNase, trypsin) (Bai et al., 2014; Bernhard et al., 2017; Bracey et al., 2019a, 2018; Bracey et al., 2019b; Cunniffe et al., 2015; De Peppo et al., 2013; Fenelon et al., 2020; Gardin et al., 2015; Gawlitta et al., 2015; He et al., 2020a, b; Inglis et al., 2019; Leng et al., 2020; Marcos-Campos et al., 2012; Mohiuddin et al., 2019; Nakamura et al., 2019, 2020; Qiu et al., 2020; Sawkins et al., 2013) with the use of detergents (i.e. SDS, Tritonx-100, EDTA). Some authors reported combined protocols that the use of an enzymatic method and chemical method (Alom et al., 2018; Emami et al., 2020; Fröhlich et al., 2010; Grayson et al., 2008; Guo et al., 2020; Lau et al., 2019; Liu et al., 2018; Marolt et al., 2012; Nie et al., 2020; Paduano et al., 2017; Qing et al., 2019; Sladkova et al., 2019; You et al., 2018; Zheng et al., 2018). Other research was reported simplified methods that involve the use of a singular category of decellularization agent, such as chemical methods by detergent (Anisimova et al., 2015; Burgkart et al., 2014; Emami et al., 2020; Jeong et al., 2019; Kedong et al., 2014; Lee et al., 2020; Quan et al., 2010; Yu et al., 2020). Seven studies used combined the mechanical method and detergents (Bagher et al., 2012; Emami et al., 2020; Gardin et al., 2015; Li et al., 2015; Rashmi and Amarpal, 2017; Shahabipour et al., 2013; Tran et al., 2018). 11 studies have provided commercially decellularized scaffolds (Arca et al., 2011; Borges et al., 2009; Butorina et al., 2020; Huang et al., 2017, 2012; Jeong et al., 2016; Kaempfen et al., 2015; Kim et al., 2012; Li et al., 2017; Pappalardo and Guarnieri, 2013; You et al., 2020). After the decellularization procedure, xenograft tissue was processed into different formulations: a) scaffolds made of the intact matrix (n = 50), b) hydrogel scaffolds made of ECM (n = 5) (Alom et al., 2018; Mohiuddin et al., 2019; Paduano et al., 2017; Qiu et al., 2020; Sawkins et al., 2013), c) scaffolds made of the intact matrix plus hydrogel (n = 2) (Kaempfen et al., 2015; Liu et al., 2018).

Cell populations were seeded in static/dynamic conditions into the decellularized scaffold. Also being nontoxic for xenograft-derived cultures, decellularized ECM demonstrated not only to support cell adhesion and proliferation that was confirmed via cells homogeneously distributed across the scaffold surface and cells adapted to dynamic culture environment but also to provide an inductive microenvironment for osteogenesis.

In vitro studies demonstrated that the presence of a decellularized xenograft scaffold can enhance the osteogenic differentiation, new bone formation, and mineralization of different cell types (Table 3).

The xenogeneic cellular antigens in the xenografts have been shown to evoke inflammatory responses. They cause releases of inflammatory mediators from the host and lead to the failure of xenogeneic grafts (Gilbert et al., 2009; Sykes and Sachs, 2019; Wessing et al., 2018). One of the stimulants of the immune system is nuclear material. However small amounts of DNA could be found in decellularized scaffolds (Vickers, 2017). 10 studies have examined the immune response to xenogeneic tissues by subcutaneous implantation of seeded or unseeded decellularized scaffolds, and the results have demonstrated high biocompatibility, with little to no evidence of inflammation and rejection (Anisimova et al., 2015; Cunniffe et al., 2015; Gardin et al., 2015; Grayson et al., 2008; Guo et al., 2020; He et al., 2020b; Lee et al., 2020; Leng et al., 2020; Qing et al., 2019; Zheng et al., 2018). Therefore, despite the presence of this residual, probably the amount of these components are not enough to induce an immunological reaction. Neutrophils are the first cells that infiltrate the implanted grafts and then they replace with macrophages (Vickers, 2017). The presence of these cells, especially mononuclear macrophages, is correlated with tissue formation in implanted scaffolds (Brown et al., 2009; Varol et al., 2015; Walsh et al., 2018). Yu et al. (2020) investigated the effects of M2 macrophages in bone formation. The results of this study indicated that the decellularized nail bed scaffolds polarized the macrophage toward the pro-regenerative M2 phenotype that directs osteogenesis by upregulation of the expression of BMP-2 (Yu et al., 2020). Activated M2 macrophages contribute to anti-inflammatory responses by participating in the clearance of remains, the suppression of inflammation and

Table 4
Outcomes reported from the 68 trials included in the systematic review.

Nr	Study	Bone outcome (follow-up)	Angiogenesis outcome (follow- up)	Mineralization (follow-up)
1	Abedin et al. (2018)	NA	NA	Histology (1, 2, 3, and 4 weeks)
2	Alom et al. (2018)	NA	NA	Histology
3	Anisimova et al. (2015)	NA	NA	NA
4	Arca et al. (2011)	NA	NA	Histology pNPP assay (14 and 21 days)
5	Bagher et al. (2012)	Histology X-ray (4, 8, and 12 weeks post implantation)	Histology (12 weeks)	Histology
6	Bai et al. (2014)	Histology (4, 8, 12 and 16 weeks postsurgery) Bone volume	Histology (16 weeks postsurgery)	X-ray (4 and 6 weeks postsurgery) µ-CT
7	Bernhard et al. (2017)	Histology Gene expression profiling (1, 3, 6, 9 and 12 weeks)	NA	Histology (1, 3, 6, 9 and 12 weeks post implantation)
8	Borges et al. (2009)	Histology Connective tissue Histomorphometry X-ray (8 and 16 weeks post implantation)	NA	NA
9	Bracey et al. (2018)	NA	NA	NA
10	Bracey et al. (2019a)	Histology & IHC Bone volume & density Gene expression profiling (4 weeks post implantation)	Histology & IHC (4 weeks post implantation)	Histology
11	Bracey et al. (2019b)	NA	NA	NA
12	Burgkart et al. (2014)	NA	NA	Histology
13	Butorina et al. (2020)	NA	NA	Histology (12 and 28 days)
14	Chen et al. (2015)	NA	NA	NA
15	Chen et al. (2010)	X-ray Histology ^{99m} TcMDP (2, 4, 8, and 12 weeks)	SPECT (2, 4, 8, and 12 weeks)	NA
16	Cunnife et al. (2015)	Histology Bone volume (4 and 8 weeks post implantation)	Histology (4 and 8 weeks post implantation)	Histology & IHC
17	De Peppo et al. (2013)	Bone volume & density Histology (3, 8, and 12 weeks) (*in vitro*) Microarray analysis Connective tissue Histomorphometry (12 weeks post implantation)	Histology (12 weeks post implantation)	Histology µ-CT (BMD) (3, 8, and 12 weeks)
Nr	Study	Bone outcome (follow-up)	Angiogenesis outcome (follow- up)	Mineralization (follow-up)
18	Elkhateb et al. (2018)	Histology & IHC (4 weeks)	Histology (4 weeks)	NA
19	Emami et al. (2020)	NA	NA	NA
20	Fénelon et al. (2020)	Bone volume Histology (1 week and one month after implantation)	Histology Histomorphometric analysis (1 week and one month after implantation)	Histology (*in vitro*) (1, 2, and 3 weeks)
21	Ferro et al. (2012)	Histology Immunofluorescence X-ray Gene expression profiling (3 months and 1 year)	NA	Histology
22	Fröhlich et al. (2010)	NA	NA	Histology & IHC Bone volume (4 and 5 weeks)
23	Gardin et al. (2015)	Histology Connective tissue (15 and 30 days)	Histology (30 days)	NA
24	Gawlitta et al. (2015)	Histology X-ray (3 and 8 weeks post implantation)	NA	Histology X-ray
25	Grayson et al. (2008)	NA	NA	Histology & IHC µ-CT (BMD) SEM (5 weeks)
26	Guo et al. (2020)	Histology & IHC Bone volume (4 and 8 weeks)	NA	NA
27	He et al. (2020b)	NA	NA	Histology
28	He et al. (2020a)	Histology Bone volume & density (4, 8, and 12 weeks)	NA	NA
29	Huang et al. (2012)	Bone volume Histology & IHC (4 months after implantation)	Histology (1, 2, and 4 months after implantation)	NA
30	Huang et al. (2017)	Histomorphometry & histology Bone volume & density CLSM (8 and 16 weeks post implantation)	Histology (8 and 16 weeks post implantation)	µ-CT CLSM MAR (8 and 16 weeks post implantation)
31	Inglis et al. (2019)	Histology & IHC Bone volume & density (8 days)	Histology	NA
32	Jeong et al. (2016)	Histology Bone volume (16 weeks)	NA	NA

(*continued on next page*)

Table 4 (*continued*)

Nr	Study	Bone outcome (follow-up)	Angiogenesis outcome (follow- up)	Mineralization (follow-up)
33	Jeong et al. (2019)	NA	NA	NA
Nr	Study	Bone outcome (follow-up)	Angiogenesis outcome (follow- up)	Mineralization (follow-up)
34	Kaempfen et al. (2015)	NA	Histology (6 weeks post implantation)	Histology X-ray µ-CT (12 weeks post implantation)
35	Kedong et al. (2014)	NA	NA	Histology
36	Kim HJ et al. (2012)	Bone volume Histology & IHC Histomorphometry (4 and 8 weeks)	Histology (4 and 8 weeks)	µ-CT (4 and 8 weeks)
37	Lau et al. (2019)	Bone volume Histology Gene expression profiling (2 and 6 weeks)	NA	Histology (1, 2, and 3 weeks)
38	Lee et al. (2014)	Histology MAR assay µ-CT(12 weeks)	NA	Histology (1, 2, and 3 weeks)
39	Lee et al. (2016)	Bone volume Histology MAR assay (12 weeks)	NA	Histology (10, 17, and 28 days)
40	Lee et al. (2020)	Bone volume & density Histology & IHC (2, 4, 6, and 8 weeks)	NA	Histology (*in vitro*) (2 and 4 weeks) Micro-CT (BMD) (4, 6, and 8 weeks post implantation)
41	Leng et al. (2020)	Histology & IHC X-ray Connective tissue (4, 8 and 12 weeks)	Histology (6, 8, and 12 weeks)	NA
42	Li et al. (2017)	Histology & IHC Gene expression profiling (4 and 8 weeks)	IHC	Histology
43	Li et al. (2015)	Bone volume & density Histology X-ray (6 weeks post implantation)	NA	Histology (*in vitro*) (3 weeks) X-ray (6 weeks post implantation)
44	Lin et al. (2018)	Bone volume & density (*in vivo*) (3, 6, and 9 weeks)	NA	Bone volume (*in vitro*) Histology EDX AFM (4 and 8 weeks)
45	Liu et al. (2018)	NA	Histology & IHC (3 weeks)	NA
46	Marcos et al. (2012)	Bone volume & density Gene expression profiling (5 weeks)	NA	IHC Bone volume and density (5 weeks)
Nr	Study	Bone outcome (follow-up)	Angiogenesis outcome (follow- up)	Mineralization (follow-up)
47	Marolt et al. (2012)	Bone volume & density Histology (*in vitro*) (5 weeks) and (8 weeks post implantation) Connective tissue	Histology (8 weeks post implantation)	Histology (*in vitro*) (3 and 5 weeks) µ-CT (BMD) (*in vitro*) (5 weeks) and (8 weeks post implantation)
48	Mohiuddin et al. (2019)	Bone volume & density IHC (6 and 12 weeks after surgery)	NA	Histology & IHC (6 and 12 weeks after surgery)
49	Nakamura et al. (2019)	NA	Micro-CT Angiography Histology (4 and 8 weeks)	Histology
50	Nakamura et al. (2020)	NA	NA	NA
51	Nie et al. (2020)	NA	NA	Histology
52	Paduano et al. (2017)	NA	NA	Histology
53	Pappalardo et al. (2013)	NA	NA	X-ray microanalysis (2 and 5 weeks)
54	Pennington et al. (2015)	Histology Bone volume (3 and 8 weeks)	NA	Histology
55	Qing et al. (2019)	Histology Gene expression profiling Western blot assay (2, 3, 4 and 5 weeks)	NA	NA
56	Qiu et al. (2020)	Bone volume & density Histology Gene expression profiling Immunofluorescent (4 and 8 weeks post implantation)	Histology & IHC (3, 7, and 21 days)	TEM (*in vitro*) Micro-CT (BMD)
57	Quan et al. (2010)	NA	NA	NA
58	Rashmi et al. (2017)	NA	NA	NA
59	Sawkins et al. (2013)	NA	NA	NA
60	Shahabipour et al. (2013)	NA	NA	NA
61	Sladkova et al. (2019)	Histology & IHC Gene expression profiling (5 weeks)	NA	Bone volume & density (5 weeks)
62	Smith et al. (2015)	NA	NA	NA
63	Smith et al. (2017)	NA	NA	XRD XRF µ-CT (2 and 4 weeks)

(*continued on next page*)

Table 4 (*continued*)

Nr	Study	Bone outcome (follow-up)	Angiogenesis outcome (follow- up)	Mineralization (follow-up)
64	Tran et al. (2019)	NA	NA	NA
65	You et al. (2018)	NA	NA	NA
66	You et al. (2020)	Histology Connective tissue (4 weeks post implantation)	NA	Histology (4 weeks post implantation)
67	Yu et al. (2020)	Histology Bone volume & density Immunofluorescent staining Western blot assay (2, 4 and 8 weeks)	NA	Histology (2, 4, and 8 weeks)
Nr	Study	Bone outcome (follow-up)	Angiogenesis outcome (follow- up)	Mineralization (follow-up)
68	Zheng et al., 2018	Histology Bone volume & density Double fluorescence labeling (6 and 12 weeks post implantation)	Micro-CT Angiography (6 and 12 weeks post implantation)	Micro-CT

NA: not available, IHC: Immunohistochemistry, AFM: Atomic Force Microscopy, EDX: Energy-dispersive X-ray spectroscopy, μ-CT: Microcomputed tomography, XRD: X-ray diffraction, XRF: X-ray fluorescence, MAR: Mineral apposition rate, SEM: Scanning electron microscope, CLSM: confocal laser scanning microscopy, SPECT: single photon emission computerized tomography, ^{99m} TcMDP: Technetium (^{99m}Tc) medronic acid, BMD: bone mineral density.

the regulation of angiogenesis. In this way, they improve graft-host connective tissue integration rather than rejection (Lucas et al., 2010; Weaver et al., 2015). Qiu et al. (2020) also demonstrated the role of M2 macrophages in a series of processes occurring during bone regeneration. They indicated that recruited macrophages, promoted angiogenesis, guided osteogenic differentiation, stimulated calcium deposition and contributed to mineralization (Qiu et al., 2020). When the immune responses to the graft of acellular sheep periosteum (AP) were compared with fresh sheep periosteum (FP), the results showed unlike FP, AP did not provoke a severe immunogenic response via the Th1 pathway (He et al., 2020b).

Alpha-Gal is a carbohydrate found in most mammalian cell membranes, except human and higher primates, and can lead to hyperacute rejection of the xenograft tissues (Abdel-Motal et al., 2009). Three studies have focused on the alpha-Gal epitope (one study *in vitro* and two studies *in vivo*). Bracey et al. (2019b) employed a decellularization protocol that removed 98.5 % of the alpha-Gal epitopes (Bracey et al., 2019b). The amount of alpha-Gal epitopes reduced about 80 % after decellularization (He et al., 2020b). Leng et al. (2020) also used immunohistochemistry to detect the alpha-Gal epitope and no alpha-Gal antigen-positive expression was observed in the decellularized bone matrix of the pig (Leng et al., 2020). Overall results demonstrate that decellularization can reduce immune response. It may explain the better bone regeneration of decellularized scaffold (Alom et al., 2018; Bagher et al., 2012; Bai et al., 2014; Bernhard et al., 2017; Borges et al., 2009; Bracey et al., 2019a; Cunniffe et al., 2015; De Peppo et al., 2013; Fenelon et al., 2020; Gardin et al., 2015; Gawlitta et al., 2015; Guo et al., 2020; He et al., 2020a; Huang et al., 2017, 2012; Inglis et al., 2019; Jeong et al., 2016; Kim et al., 2012; Lau et al., 2019; Lee et al., 2020; Leng et al., 2020; Li et al., 2017, 2015; Marcos-Campos et al., 2012; Marolt et al., 2012; Mohiuddin et al., 2019; Qing et al., 2019; Qiu et al., 2020; You et al., 2020; Yu et al., 2020; Zheng et al., 2018) (Table 4).

Angiogenesis is an indispensable feature for graft survival, integration, and function, since plays a vital role in supplying cells with oxygen and nutrients (Lin et al., 2016). Three studies have attempted to enhance the establishment of vascular networks within scaffold for bone regeneration. It has been shown that the sequential seeding of human smooth muscle cells and human umbilical vein endothelial cells enhanced the generation of early microvascular networks, which could further support the *in vitro* tissue engineering of bone grafts (Liu et al., 2018; Marcelo et al., 2013). Kaempfen et al. (2015) introduced a novel treatment based on pre-vascularization. They implanted the BMSC-seeded scaffold and the surrounding vasculature into the orthopic site and indicated that this method of pre-vascularization could not avoid tissue-necrosis in the orthopic site (Kaempfen et al., 2015). The subcutaneous implantation of decellularized cancellous bones (DCBs) into mice indicated that DCBs were recellularized by some host cells and induced hematopoiesis, regardless of pre-addition of hMSCs into the matrix. The results of this study showed that reticular and adipose cells recellularized DCBs, at the original cellular location and DCBs enhanced homing of hematopoietic stem cells. This study suggested the reticular tissues are stimulating the hematopoiesis into the DCBs (Nakamura et al., 2019). Other studies reported the formation of the vascular network within the scaffold; vascularization could contribute to the bone healing process *in vivo* (Bagher et al., 2012; Bai et al., 2014; Bracey et al., 2019a; Fenelon et al., 2020; Gardin et al., 2015; Huang et al., 2017, 2012; Inglis et al., 2019; Kim et al., 2012; Leng et al., 2020; Li et al., 2017; Marolt et al., 2012; Qiu et al., 2020; Zheng et al., 2018) (Table 4).

4. Discussion

Many types of research aim to create bone graft substitutes, therefore a systematic study of bone graft characteristics is important for future research directions and the preoperative planning of implant selection. More recently, due to the COVID-19 pandemic and the lack of knowledge about the consequences of this disease on the availability and the risk of disease transmission of allografts, decellularized tissues can be considered as a safe and promising prospect. The purpose of this paper is to systematically review the quality of decellularized xenograft and allograft scaffolds for the production of bone substitutes by using the PRISMA guidelines. Of the 484 reviewed papers, 68 were eligible for this study and were analyzed to obtain a clear outcome. On the other hand, the included studies were extremely heterogeneous and could not be quantitatively assessed. Therefore, the results were expressed descriptively.

In the majority of the studies in this systematic review, the natural bone was used as a scaffold due to the appropriate composition, specific microstructure, biomechanics, and exhibited strong osteogenic characterizes for bone development and regeneration. The clinical exploitation of decellularized bone was limited due to the lack of a suitable sterilization method and possibly compromises the integrity and function of the implant (Fidalgo et al., 2018). An ideal decellularization method should remove all cellular components without any change in mechanical and biological properties of the native bone, in consequence, supporting the cellular function, cell interaction, as well as cell differentiation.

For bone regeneration, different allograft strategies have been used such as decellularized bone matrix, demineralized bone matrix, or other human tissues. Five studies that were included in this review used human bone as a decellularized scaffold (Abedin et al., 2018; Ferro et al., 2012; Sladkova et al., 2019; Smith et al., 2017, 2015). Two of them designed a novel decellularization method based on wash centrifuge phases to remove the marrow materials (Smith et al., 2017, 2015). They showed that the chemicals materials in the washing method did not negatively affect ECM proteins and growth factors, science MSCs that were seeded into the scaffold, had been differentiated to osteogenic lineage (Smith et al., 2017, 2015). In this paper, some studies examined soft tissues such as acellular human dermis extracellular matrix (ADM) (Borges et al., 2009; Jeong et al., 2016; Kim et al., 2012; Pappalardo and Guarnieri, 2013), decellularized human amniotic membrane (HAM) (Fenelon et al., 2020; Li et al., 2015), decellularized blood vessels from the human placenta (Inglis et al., 2019), and decellularized human hydrogel treated adipose tissue (Mohiuddin et al., 2019) as a scaffold for bone tissue engineering purposes. These scaffolds have demonstrated the integration of decellularized grafts with higher levels of bone formation than the control group (without the grafts). Although commonly soft decellularized matrices are utilized for soft tissue defects, but these models provide a new approach to the integration of these scaffolds with the bone periosteum and growth factor homeostasis (Inglis et al., 2019; Marcelo et al., 2013; Mohiuddin et al., 2019).

The first transplantation of xenograft was reported in 1668 (Deschamps et al., 2005). Since then, lots of researches have been designed and published, but those outcomes mostly were not successful, because of the limitation of grafts, immune response, and rejection (Elliot and Richards, 2011). The possibilities of using acellular xenogeneic bone scaffolds in clinical applications depend on the immune system's acceptance (El-Rashidy et al., 2017), and a series of cascade reactions to repair bone damage (Pearce et al., 2007). Xenografts have been used in several studies to serve as a scaffold to repair bone defects. About 36 studies used cancellous bone. Cancellous bone has consisted about 20 % of mature bone (Sikavitsas et al., 2001), and decellularized cancellous bone is widely used as a bone graft substitute because it acts as a load-bearing structure, mimics the basic mechanical properties of bone and this structure is maintained until the voids filled and remodeled by host ingrowth (Hutmacher, 2000; Schwiedrzik et al., 2011). Without appropriate stiffness and strength at the graft site, the scaffold may be resorbed by the host body (Liu et al., 2013). It can be tested whether the scaffold maintained osteoconductivity as a graft or not based on the differentiation of stem cells into the osteoblast. These results can be confirmed by mineralization and expression ALP and bone-specific genes which were reported by some studies. Although it has been reported that, stiffness of the scaffold affects stem cell fate and seems that softer matrices direct the cells to neurogenic lineages and the sifter matrices promote differentiation stem cells to osteogenic lineages (Watari et al., 2012), but we have shown that the demineralized and decellularized human 3D epiphyseal bone scaffold induces osteogenic differentiation and bone mineralization even in the standard culture medium. Therefore, it has the potential to be used as a bone graft without the need for bone induction agents (Abedin et al., 2018). Since the addition of each factor may have undesired effects, reducing the number of parameters involved in differentiation can lead to more controlled conditions (Heydari Asl et al., 2018). Therefore, matrix stiffness is not necessarily a criterion for graft success. Another reason that used cancellous bone is its high-porosity with a porosity of 50%–90% (Salgado et al., 2004). The porosity and pore size are two main properties of bone scaffold and have been reported to facilitate the spread and adhesion of cells into the scaffold and affect the mechanical strength of the scaffold (Bertoldi et al., 2011). Porosity also is an important factor for anxiolysis and provided adequate space for vessels (Byrne et al., 2007). In these aspects, the cancellous bone appears to be a reasonable bone scaffold candidate.

Overall results of this study show that the structures and characteristics of xenograft scaffold promote capillary ingrowth and migration and proliferation of osteoblasts and also have been confirmed biocompatible and osteoconductive. In the present study, decellularized xenograft cancellous bone has been suggested as the best alternative for autografts. Decellularized allografts are less operative compared to decellularized xenograft due to limited availability and the exorbitant cost of one milliliter of DBM (Stancoven et al., 2013) and thus, mass production of decellularized scaffolds from human sources is hard to be reached. On the other hand, although great progress has been reported in the literature about decellularization and *in vitro* recellularization of human and animal bone tissues, extensive research is still needed to clear the advanced outcomes of *in vivo* implantation.

5. Conclusion

Decellularized xenograft or allograft bone scaffolds provide a unique natural microstructure that not only has comparable stiffness to human bone tissue but also has similar components, porosity and pore size, which can promote osteoinduction and osteogenesis, resulting in bone mineralization. It is a promising method for bone grafting that can overcome many problems of transplantation, including rejection, and disease transmission. Based on this review, the decellularized xenograft cancellous bone appears to be the best alternative to autograft, as this scaffold promotes capillary ingrowth, migration and proliferation of osteoblasts, and osteogenesis. Availability, affordability and the capability of producing a wide variety of geometric shapes of this scaffold make it suitable for mass production. However, there is limited research on *in vivo* implantation of decellularized xenograft cancellous bone. Standardization and quantitative analysis of the outcome of decellularized xenograft bone are yet to be done.

Appendix A. Supplementary data

Supplementary material related to this article can be found, in the online version, at doi:https://doi.org/10.1016/j.tice.2021.101494.

References

Abdel-Motal, U.M., Wigglesworth, K., Galili, U., 2009. Mechanism for increased immunogenicity of vaccines that form in vivo immune complexes with the natural anti-Gal antibody. Vaccine 27, 3072–3082.

Abedin, E., Lari, R., Shahri, N.M., Fereidoni, M., 2018. Development of a demineralized and decellularized human epiphyseal bone scaffold for tissue engineering: a histological study. Tissue Cell 55, 46–52.

Alom, N., Peto, H., Kirkham, G.R., Shakesheff, K.M., White, L.J., 2018. Bone extracellular matrix hydrogel enhances osteogenic differentiation of C2C12 myoblasts and mouse primary calvarial cells. J. Biomed. Mater. Res. Part B Appl. Biomater. 106, 900–908.

Anisimova, N., Kiselevsky, M., Sukhorukova, I., Shvindina, N., Shtansky, D., 2015. Fabrication method, structure, mechanical, and biological properties of decellularized extracellular matrix for replacement of wide bone tissue defects. J. Mech. Behav. Biomed. Mater. 49, 255–268.

Arca, T., Proffitt, J., Genever, P., 2011. Generating 3D tissue constructs with mesenchymal stem cells and a cancellous bone graft for orthopaedic applications. Biomed. Mater. 6, 025006.

Armiento, A., Stoddart, M., Alini, M., Eglin, D., 2018. Biomaterials for articular cartilage tissue engineering: learning from biology. Acta Biomater. 65, 1–20.

Bagher, Z., Rajaei, F., Shokrgozar, M., 2012. Comparative study of bone repair using porous hydroxyapatite/β-tricalcium phosphate and xenograft scaffold in rabbits with tibia defect. Iran. Biomed. J. 16, 18.

Bai, M., Zhang, T., Ling, T., Zhou, Z., Xie, H., Zhang, W., Hu, G., Jiang, C., Li, M., Feng, B., 2014. Guided bone regeneration using acellular bovine pericardium in a rabbit mandibular model: in-vitro and in-vivo studies. J. Periodont. Res. 49, 499–507.

Benders, K.E., van Weeren, P.R., Badylak, S.F., Saris, D.B., Dhert, W.J., Malda, J., 2013. Extracellular matrix scaffolds for cartilage and bone regeneration. Trends Biotechnol. 31, 169–176.

Bernhard, J., Ferguson, J., Rieder, B., Heimel, P., Nau, T., Tangl, S., Redl, H., Vunjak-Novakovic, G., 2017. Tissue-engineered hypertrophic chondrocyte grafts enhanced long bone repair. Biomaterials 139, 202–212.

Bertoldi, S., Fare, S., Tanzi, M.C., 2011. Assessment of scaffold porosity: the new route of micro-CT. J. Appl. Biomater. Biomech. 9, 165–175.

Bhumiratana, S., Bernhard, J.C., Alfi, D.M., Yeager, K., Eton, R.E., Bova, J., Gimble, J.M., Lopez, M.J., Eisig, S.B., Vunjak-Novakovic, G., 2016. Tissue-engineered autologous grafts for facial bone reconstruction. Sci. Transl. Med. 8, 343ra383-343ra383.

Borges, G.J., Novaes Jr., A.B., de Moraes Grisi, M.F., Palioto, D.B., Taba Jr., M., De Souza, S.L.S., 2009. Acellular dermal matrix as a barrier in guided bone regeneration: a clinical, radiographic and histomorphometric study in dogs. Clin. Oral Implants Res. 20, 1105–1115.

Bracey, D.N., Seyler, T.M., Jinnah, A.H., Lively, M.O., Willey, J.S., Smith, T.L., Van Dyke, M.E., Whitlock, P.W., 2018. A decellularized porcine xenograft-derived bone scaffold for clinical use as a bone graft substitute: a critical evaluation of processing and structure. J. Funct. Biomater. 9, 45.

Bracey, D.N., Jinnah, A.H., Willey, J.S., Seyler, T.M., Hutchinson, I.D., Whitlock, P.W., Smith, T.L., Danelson, K.A., Emory, C.L., Kerr, B.A., 2019a. Investigating the osteoinductive potential of a decellularized xenograft bone substitute. Cells Tissues Organs 207, 97–113.

Bracey, D.N., Seyler, T.M., Jinnah, A.H., Smith, T.L., Ornelles, D.A., Deora, R., Parks, G. D., Van Dyke, M.E., Whitlock, P.W., 2019b. A porcine xenograft-derived bone scaffold is a biocompatible bone graft substitute: an assessment of cytocompatibility and the alpha-Gal epitope. Xenotransplantation 26, e12534.
Brown, B.N., Valentin, J.E., Stewart-Akers, A.M., McCabe, G.P., Badylak, S.F., 2009. Macrophage phenotype and remodeling outcomes in response to biologic scaffolds with and without a cellular component. Biomaterials 30, 1482–1491.
Burgkart, R., Tron, A., Prodinger, P., Culmes, M., Tuebel, J., van Griensven, M., Saldamli, B., Schmitt, A., 2014. Decellularized kidney matrix for perfused bone engineering. Tissue Eng. Part C Methods 20, 553–561.
Butorina, N., Payushina, O., Sheveleva, O., Novokreshchenova, A., Domaratskaya, E., Istranov, L., Istranova, E., 2020. Experimental study of the possibility of culturing of mesenchymal stromal cell and induction of osteogenic differentiation on collagen-based scaffolds of various modifications. Bull. Exp. Biol. Med.
Byrne, D.P., Lacroix, D., Planell, J.A., Kelly, D.J., Prendergast, P.J., 2007. Simulation of tissue differentiation in a scaffold as a function of porosity, Young's modulus and dissolution rate: application of mechanobiological models in tissue engineering. Biomaterials 28, 5544–5554.
Calori, G.M., Mazza, E., Colombo, M., Ripamonti, C., 2011. The use of bone-graft substitutes in large bone defects: any specific needs? Injury 42 (Suppl 2), S56–63.
Chen, G., Lv, Y., 2017. Decellularized Bone Matrix Scaffold for Bone Regeneration, Decellularized Scaffolds and Organogenesis. Springer, pp. 239–254.
Chen, Q., Yang, Z., Sun, S., Huang, H., Sun, X., Wang, Z., Zhang, Y., Zhang, B., 2010. Adipose-derived stem cells modified genetically in vivo promote reconstruction of bone defects. Cytotherapy 12, 831–840.
Chen, K., Lin, X., Zhang, Q., Ni, J., Li, J., Xiao, J., Wang, Y., Ye, Y., Chen, L., Jin, K., Chen, L., 2015. Decellularized periosteum as a potential biologic scaffold for bone tissue engineering. Acta Biomater. 19, 46–55.
Cummings, L.C., Kaldahl, W.B., Allen, E.P., 2005. Histologic evaluation of autogenous connective tissue and acellular dermal matrix grafts in humans. J. Periodontol. 76, 178–186.
Cunniffe, G.M., Vinardell, T., Murphy, J.M., Thompson, E.M., Matsiko, A., O'Brien, F.J., Kelly, D.J., 2015. Porous decellularized tissue engineered hypertrophic cartilage as a scaffold for large bone defect healing. Acta Biomater. 23, 82–90.
De Peppo, G.M., Marcos-Campos, I., Kahler, D.J., Alsalman, D., Shang, L., Vunjak-Novakovic, G., Marolt, D., 2013. Engineering bone tissue substitutes from human induced pluripotent stem cells. Proc. Natl. Acad. Sci. 110, 8680–8685.
Deschamps, J.Y., Roux, F.A., Sai, P., Gouin, E., 2005. History of xenotransplantation. Xenotransplantation 12, 91–109.
Ebraheim, N.A., Elgafy, H., Xu, R., 2001. Bone-graft harvesting from iliac and fibular donor sites: techniques and complications. J. Am. Acad. Orthop. Surg. 9, 210–218.
Elkhateb, L., Zohdy, A., Atalla, S.S., Moussa, M.H., Hamam, G.G., Zahra, F.A.E.A., 2018. Comparative study on acellular dermal graft versus propylene mesh both either loaded or unloaded with BM-MSCs in healing of skull bone defect in rats: histological and immunohistochemical study. Int. J. Stem Cells 11, 216.
Elliot, R.R., Richards, R.H., 2011. Failed operative treatment in two cases of pseudarthrosis of the clavicle using internal fixation and bovine cancellous xenograft (Tutobone). J. Pediatr. Orthop. B 20, 349–353.
El-Rashidy, A., Roether, J., Harhaus, L., Kneser, U., Boccaccini, A., 2017. Regenerating bone with bioactive glass scaffolds: a review of in vivo studies in bone defect models. Acta Biomater. 62, 1.
Emami, A., Talaei-Khozani, T., Vojdani, Z., Zarei Fard, N., 2020. Comparative assessment of the efficiency of various decellularization agents for bone tissue engineering. J. Biomed. Mater. Res. Part B Appl. Biomater.
Fenelon, M., Etchebarne, M., Siadous, R., Gremare, A., Durand, M., Sentilhes, L., Torres, Y., Catros, S., Gindraux, F., L'Heureux, N., Fricain, J.C., 2020. Assessment of fresh and preserved amniotic membrane for guided bone regeneration in mice. J. Biomed. Mater. Res. A 108, 2044–2056.
Ferro, F., Spelat, R., D'Aurizio, F., Falini, G., De Pol, I., Pandolfi, M., Beltrami, A.P., Cesselli, D., Beltrami, C.A., Curcio, F., 2012. Acellular bone colonization and aggregate culture conditions diversely influence murine periosteum mesenchymal stem cell differentiation potential in long-term in vitro osteoinductive conditions. Tissue Eng. Part A 18, 1509–1519.
Fidalgo, C., Iop, L., Sciro, M., Harder, M., Mavrilas, D., Korossis, S., Bagno, A., Palù, G., Aguiari, P., Gerosa, G., 2018. A sterilization method for decellularized xenogeneic cardiovascular scaffolds. Acta Biomater. 67, 282–294.
Fröhlich, M., Grayson, W.L., Marolt, D., Gimble, J.M., Kregar-Velikonja, N., Vunjak-Novakovic, G., 2010. Bone grafts engineered from human adipose-derived stem cells in perfusion bioreactor culture. Tissue Eng. Part A 16, 179–189.
Gardin, C., Ricci, S., Ferroni, L., Guazzo, R., Sbricoli, L., De Benedictis, G., Finotti, L., Isola, M., Bressan, E., Zavan, B., 2015. Decellularization and delipidation protocols of bovine bone and pericardium for bone grafting and guided bone regeneration procedures. PLoS One 10, e0132344.
Gawlitta, D., Benders, K.E., Visser, J., van der Sar, A.S., Kempen, D.H., Theyse, L.F., Malda, J., Dhert, W.J., 2015. Decellularized cartilage-derived matrix as substrate for endochondral bone regeneration. Tissue Eng. Part A 21, 694–703.
Gilbert, T.W., Freund, J.M., Badylak, S.F., 2009. Quantification of DNA in biologic scaffold materials. J. Surg. Res. 152, 135–139.
Grayson, W.L., Bhumiratana, S., Cannizzaro, C., Chao, P.-H.G., Lennon, D.P., Caplan, A. I., Vunjak-Novakovic, G., 2008. Effects of initial seeding density and fluid perfusion rate on formation of tissue-engineered bone. Tissue Eng. Part A 14, 1809–1820.
Gruskin, E., Doll, B.A., Futrell, F.W., Schmitz, J.P., Hollinger, J.O., 2012. Demineralized bone matrix in bone repair: history and use. Adv. Drug Deliv. Rev. 64, 1063–1077.
Guo, K., Wang, W., Liu, Z., Xu, W., Zhang, S., Yang, C., 2020. Reliability of acellular decalcified and decalcified teeth as bone graft material: an experimental and pathological study in rats. Int. J. Clin. Exp. Pathol. 13, 837.
He, J., Li, Z., Yu, T., Wang, W., Tao, M., Ma, Y., Wang, S., Fan, J., Tian, X., Wang, X., 2020a. Preparation and evaluation of acellular sheep periostea for guided bone regeneration. J. Biomed. Mater. Res. A 108, 19–29.
He, J., Li, Z., Yu, T., Wang, W., Tao, M., Wang, S., Ma, Y., Fan, J., Tian, X., Wang, X., 2020b. In vitro and in vivo biocompatibility study on acellular sheep periosteum for guided bone regeneration. Biomed. Mater. 15, 015013.
Heydari Asl, S., Hosseinpoor, H., Parivar, K., Hayati Roodbari, N., Hanaee-Ahvaz, H., 2018. Physical stimulation and scaffold composition efficiently support osteogenic differentiation of mesenchymal stem cells. Tissue Cell 50, 1–7.
Ho-Shui-Ling, A., Bolander, J., Rustom, L.E., Johnson, A.W., Luyten, F.P., Picart, C., 2018. Bone regeneration strategies: engineered scaffolds, bioactive molecules and stem cells current stage and future perspectives. Biomaterials 180, 143–162.
Huang, Y.-Z., Cai, J.-Q., Xue, J., Chen, X.-H., Zhang, C.-L., Li, X.-Q., Yang, Z.-M., Huang, Y.-C., Deng, L., 2012. The poor osteoinductive capability of human acellular bone matrix. Int. J. Artif. Organs 35, 1061–1069.
Huang, R.-L., Tremp, M., Ho, C.-K., Sun, Y., Liu, K., Li, Q., 2017. Prefabrication of a functional bone graft with a pedicled periosteal flap as an in vivo bioreactor. Sci. Rep. 7, 1–11.
Hutmacher, D.W., 2000. Scaffolds in tissue engineering bone and cartilage. Biomaterials 21, 2529–2543.
Inglis, S., Schneider, K.H., Kanczler, J.M., Redl, H., Oreffo, R.O., 2019. Harnessing human decellularized blood vessel matrices and cellular construct implants to promote bone healing in an ex vivo organotypic bone defect model. Adv. Healthc. Mater. 8, 1800088.
Jeong, W.H., Roh, T.S., Kim, Y.S., Kang, E.H., Jung, B.K., Lee, W.J., Lew, D.H., Yun, I.S., 2016. Acceleration of osteogenesis by platelet-rich plasma with acellular dermal matrix in a calvarial defect model. Childs Nerv. Syst. 32, 1653–1659.
Jeong, H., Asai, J., Ushida, T., Furukawa, K.S., 2019. Assessment of the inner surface microstructure of decellularized cortical bone by a scanning Electron microscope. Bioengineering 6, 86.
Kaempfen, A., Todorov, A., Güven, S., Largo, R.D., Jaquiéry, C., Scherberich, A., Martin, I., Schaefer, D.J., 2015. Engraftment of prevascularized, tissue engineered constructs in a novel rabbit segmental bone defect model. Int. J. Mol. Sci. 16, 12616–12630.
Kedong, S., Wenfang, L., Yanxia, Z., Hong, W., Ze, Y., Mayasari, L., Tianqing, L., 2014. Dynamic fabrication of tissue-engineered bone substitutes based on derived cancellous bone scaffold in a spinner flask bioreactor system. Appl. Biochem. Biotechnol. 174, 1331–1343.
Kim, H.J., Park, S.S., Oh, S.Y., Kim, H., Kweon, O.K., Woo, H.M., Kim, W.H., 2012. Effect of acellular dermal matrix as a delivery carrier of adipose-derived mesenchymal stem cells on bone regeneration. J. Biomed. Mater. Res. B Appl. Biomater. 100, 1645–1653.
Kon, E., Filardo, G., Brittberg, M., Busacca, M., Condello, V., Engebretsen, L., Marlovits, S., Niemeyer, P., Platzer, P., Posthumus, M., Verdonk, P., Verdonk, R., Victor, J., van der Merwe, W., Widuchowski, W., Zorzi, C., Marcacci, M., 2018. A multilayer biomaterial for osteochondral regeneration shows superiority vs microfractures for the treatment of osteochondral lesions in a multicentre randomized trial at 2 years. Knee Surg. Sports Traumatol. Arthrosc. 26, 2704–2715.
Konofaos, P., Kashyap, A., Ver Halen, J., 2014. Biomedical approaches to improve bone healing in distraction osteogenesis: a current update and review. Biomed. Tech. (Berl) 59, 177–183.
Lau, C.S., Hassanbhai, A., Wen, F., Wang, D., Chanchareonsook, N., Goh, B.T., Yu, N., Teoh, S.H., 2019. Evaluation of decellularized tilapia skin as a tissue engineering scaffold. J. Tissue Eng. Regen. Med. 13, 1779–1791.
Lee, D.J., Padilla, R., Zhang, H., Hu, W.S., Ko, C.C., 2014. Biological assessment of a calcium silicate incorporated hydroxyapatite-gelatin nanocomposite: a comparison to decellularized bone matrix. Biomed Res. Int. 2014, 837524.
Lee, D.J., Diachina, S., Lee, Y.T., Zhao, L., Zou, R., Tang, N., Han, H., Chen, X., Ko, C.C., 2016. Decellularized bone matrix grafts for calvaria regeneration. J. Tissue Eng. 7, 2041731416680306.
Lee, M.S., Lee, D.H., Jeon, J., Tae, G., Shin, Y.M., Yang, H.S., 2020. Biofabrication and application of decellularized bone extracellular matrix for effective bone regeneration. J. Ind. Eng. Chem. 83, 323–332.
Leng, Y., Ren, G., Cui, Y., Peng, C., Wang, J., Wu, D., Liu, H., 2020. Platelet-rich plasma-enhanced osseointegration of decellularized bone matrix in critical-size radial defects in rabbits. Ann. Transl. Med. 8.
Li, W., Ma, G., Brazile, B., Li, N., Dai, W., Butler, J.R., Claude, A.A., Wertheim, J.A., Liao, J., Wang, B., 2015. Investigating the potential of amnion-based scaffolds as a barrier membrane for guided bone regeneration. Langmuir 31, 8642–8653.
Li, M., Zhang, C., Cheng, M., Gu, Q., Zhao, J., 2017. Small intestinal submucosa: a potential osteoconductive and osteoinductive biomaterial for bone tissue engineering. Mater. Sci. Eng. C 75, 149–156.
Lin, Y., Xiao, W., Bal, B.S., Rahaman, M.N., 2016. Effect of copper-doped silicate 13–93 bioactive glass scaffolds on the response of MC3T3-E1 cells in vitro and on bone regeneration and angiogenesis in rat calvarial defects in vivo. Mater. Sci. Eng. C 67, 440–452.
Lin, X., Zhao, C., Zhu, P., Chen, J., Yu, H., Cai, Y., Zhang, Q., Qin, A., Fan, S., 2018. Periosteum extracellular-matrix-mediated acellular mineralization during bone formation. Adv. Healthc. Mater. 7, 1700660.
Liu, M., Lv, Y., 2018. Reconstructing bone with natural bone graft: a review of in vivo studies in bone defect animal model. Nanomaterials (Basel, Switzerland) 8, 999.
Liu, Y., Lim, J., Teoh, S.H., 2013. Review: development of clinically relevant scaffolds for vascularised bone tissue engineering. Biotechnol. Adv. 31, 688–705.
Liu, X., Jakus, A.E., Kural, M., Qian, H., Engler, A., Ghaedi, M., Shah, R., Steinbacher, D. M., Niklason, L.E., 2018. Vascularization of natural and synthetic bone scaffolds. Cell Transplant. 27, 1269–1280.

Lucas, T., Waisman, A., Ranjan, R., Roes, J., Krieg, T., Müller, W., Roers, A., Eming, S.A., 2010. Differential roles of macrophages in diverse phases of skin repair. J. Immunol. 184, 3964–3977.
Lumpkins, S.B., Pierre, N., McFetridge, P.S., 2008. A mechanical evaluation of three decellularization methods in the design of a xenogeneic scaffold for tissue engineering the temporomandibular joint disc. Acta Biomater. 4, 808–816.
Ma, R., Li, M., Luo, J., Yu, H., Sun, Y., Cheng, S., Cui, P., 2013. Structural integrity, ECM components and immunogenicity of decellularized laryngeal scaffold with preserved cartilage. Biomaterials 34, 1790–1798.
Marcelo, K.L., Goldie, L.C., Hirschi, K.K., 2013. Regulation of endothelial cell differentiation and specification. Circ. Res. 112, 1272–1287.
Marcos-Campos, I., Marolt, D., Petridis, P., Bhumiratana, S., Schmidt, D., Vunjak-Novakovic, G., 2012. Bone scaffold architecture modulates the development of mineralized bone matrix by human embryonic stem cells. Biomaterials 33, 8329–8342.
Marolt, D., Campos, I.M., Bhumiratana, S., Koren, A., Petridis, P., Zhang, G., Spitalnik, P. F., Grayson, W.L., Vunjak-Novakovic, G., 2012. Engineering bone tissue from human embryonic stem cells. Proc. Natl. Acad. Sci. 109, 8705–8709.
Mishra, R., Bishop, T., Valerio, I.L., Fisher, J.P., Dean, D., 2016. The potential impact of bone tissue engineering in the clinic. Regen. Med. 11, 571–587.
Moher, D., Shamseer, L., Clarke, M., Ghersi, D., Liberati, A., Petticrew, M., Shekelle, P., Stewart, L.A., 2015. Preferred reporting items for systematic review and meta-analysis protocols (PRISMA-P) 2015 statement. Syst. Rev. 4, 1.
Mohiuddin, O.A., Campbell, B., Poche, J.N., Ma, M., Rogers, E., Gaupp, D., Harrison, M. A., Bunnell, B.A., Hayes, D.J., Gimble, J.M., 2019. Decellularized adipose tissue hydrogel promotes bone regeneration in critical-sized mouse femoral defect model. Front. Bioeng. Biotechnol. 7, 211.
Nakamura, N., Kimura, T., Nam, K., Fujisato, T., Iwata, H., Tsuji, T., Kishida, A., 2019. Induction of in vivo ectopic hematopoiesis by a three-dimensional structured extracellular matrix derived from decellularized cancellous bone. ACS Biomater. Sci. Eng. 5, 5669–5680.
Nakamura, N., Saito, K., Kimura, T., Kishida, A., 2020. Recellularization of decellularized cancellous bone scaffolds using low-temperature cell seeding. Tissue Cell 101385.
Nie, X., Wang, D.A., 2018. Decellularized orthopaedic tissue-engineered grafts: biomaterial scaffolds synthesised by therapeutic cells. Biomater. Sci. 6, 2798–2811.
Nie, Z., Wang, X., Ren, L., Kang, Y., 2020. Development of a decellularized porcine bone matrix for potential applications in bone tissue regeneration. Regen. Med.
Paduano, F., Marrelli, M., Alom, N., Amer, M., White, L.J., Shakesheff, K.M., Tatullo, M., 2017. Decellularized bone extracellular matrix and human dental pulp stem cells as a construct for bone regeneration. J. Biomater. Sci. Polym. Ed. 28, 730–748.
Pappalardo, S., Guarnieri, R., 2013. Proliferation assessment of mesenchymal stem cells on an acellular dermal matrix (AlloDerm® GBR) used for guided bone regeneration. J. Biomater. Tissue Eng. 3, 589–596.
Pearce, A.I., Richards, R.G., Milz, S., Schneider, E., Pearce, S.G., 2007. Animal models for implant biomaterial research in bone: a review. Eur. Cell. Mater. 13, 1–10.
Pennington, E.C., Dionigi, B., Gray, F.L., Ahmed, A., Brazzo, J., Dolinko, A., Calderon, N., Darrah, T., Zurakowski, D., Nazarian, A., Snyder, B., Fauza, D.O., 2015. Limb reconstruction with decellularized, non-demineralized bone in a young leporine model. Biomed. Mater. 10, 015021.
Pirnay, J.P., Baudoux, E., Cornu, O., Delforge, A., Delloye, C., Guns, J., Heinen, E., Van den Abbeel, E., Vanderkelen, A., Van Geyt, C., 2015. Access to human tissues for research and product development: from EU regulation to alarming legal developments in Belgium. EMBO Rep. 16, 557–562.
Qing, Q., Zhang, Y.J., Yang, J.L., Ning, L.J., Zhang, Y.J., Jiang, Y.L., Zhang, Y., Luo, J.C., Qin, T.W., 2019. Effects of hydrogen peroxide on biological characteristics and osteoinductivity of decellularized and demineralized bone matrices. J. Biomed. Mater. Res. A 107, 1476–1490.
Qiu, P., Li, M., Chen, K., Fang, B., Chen, P., Tang, Z., Lin, X., Fan, S., 2020. Periosteal matrix-derived hydrogel promotes bone repair through an early immune regulation coupled with enhanced angio-and osteogenesis. Biomaterials 227, 119552.
Quan, T.M., Thanh, T.T., Ngoc, P.K., Ha, T.L.B., 2010. Study on artificial scaffold from cancellous bone. In: The Third International Conference on the Development of Biomedical Engineering in Vietnam. Springer, pp. 152–154.
Raghuram, A., Singh, A., Chang, D.K., Nunez, M., Reece, E.M., 2019. Bone grafts, bone substitutes, and orthobiologics: applications in plastic surgery. Semin. Plast. Surg. 33, 190–199.
Rashmi, R.P., Amarpal, H., 2017. Evaluation of tissue-engineered bone constructs using rabbit fetal osteoblasts on acellular bovine cancellous bone matrix. Vet. World 10, 163.
Roddy, E., DeBaun, M.R., Daoud-Gray, A., Yang, Y.P., Gardner, M.J., 2018. Treatment of critical-sized bone defects: clinical and tissue engineering perspectives. Eur. J. Orthop. Surg. Traumatol. 28, 351–362.
Roseti, L., Parisi, V., Petretta, M., Cavallo, C., Desando, G., Bartolotti, I., Grigolo, B., 2017. Scaffolds for bone tissue engineering: state of the art and new perspectives. Mater. Sci. Eng. C 78, 1246–1262.
Salgado, A.J., Coutinho, O.P., Reis, R.L., 2004. Bone tissue engineering: state of the art and future trends. Macromol. Biosci. 4, 743–765.
Sawkins, M.J., Bowen, W., Dhadda, P., Markides, H., Sidney, L.E., Taylor, A.J., Rose, F. R., Badylak, S.F., Shakesheff, K.M., White, L.J., 2013. Hydrogels derived from demineralized and decellularized bone extracellular matrix. Acta Biomater. 9, 7865–7873.
Schenke-Layland, K., Nerem, R.M., 2011. In vitro human tissue models–moving towards personalized regenerative medicine. Adv. Drug Deliv. Rev. 63, 195–196.
Schwiedrzik, J.J., Kaudela, K.H., Burner, U., Zysset, P.K., 2011. Fabric-mechanical property relationships of trabecular bone allografts are altered by supercritical CO (2) treatment and gamma sterilization. Bone 48, 1370–1377.
Seyler, T.M., Bracey, D.N., Plate, J.F., Lively, M.O., Mannava, S., Smith, T.L., Saul, J.M., Poehling, G.G., Van Dyke, M.E., Whitlock, P.W., 2017. The development of a xenograft-derived scaffold for tendon and ligament reconstruction using a decellularization and oxidation protocol. Arthroscopy 33, 374–386.
Shahabipour, F., Mahdavi-Shahri, N., Matin, M.M., Tavassoli, A., Zebarjad, S.M., 2013. Scaffolds derived from cancellous bovine bone support mesenchymal stem cells' maintenance and growth. In Vitro Cell. Dev. Biol. Anim. 49, 440–448.
Sikavitsas, V.I., Temenoff, J.S., Mikos, A.G., 2001. Biomaterials and bone mechanotransduction. Biomaterials 22, 2581–2593.
Sladkova, M., Cheng, J., Palmer, M., Chen, S., Lin, C., Xia, W., Yu, Y.E., Zhou, B., Engqvist, H., de Peppo, G.M., 2019. Comparison of decellularized cow and human bone for engineering bone grafts with human induced pluripotent stem cells. Tissue Eng. Part A 25, 288–301.
Smith, C.A., Richardson, S.M., Eagle, M.J., Rooney, P., Board, T., Hoyland, J.A., 2015. The use of a novel bone allograft wash process to generate a biocompatible, mechanically stable and osteoinductive biological scaffold for use in bone tissue engineering. J. Tissue Eng. Regen. Med. 9, 595–604.
Smith, C.A., Board, T.N., Rooney, P., Eagle, M.J., Richardson, S.M., Hoyland, J.A., 2017. Correction: human decellularized bone scaffolds from aged donors show improved osteoinductive capacity compared to young donor bone. PLoS One 12, e0187783.
Stancoven, B.W., Lee, J., Dixon, D.R., McPherson 3rd, J.C., Bisch, F.C., Wikesjo, U.M., Susin, C., 2013. Effect of bone morphogenetic protein-2, demineralized bone matrix and systemic parathyroid hormone (1-34) on local bone formation in a rat calvaria critical-size defect model. J. Periodontal Res. 48, 243–251.
Sykes, M., Sachs, D.H., 2019. Transplanting organs from pigs to humans. Sci. Immunol. 4, eaau6298.
Tabata, Y., 2009. Biomaterial technology for tissue engineering applications. J. R. Soc. Interface 6 (Suppl 3), S311–324.
Tapias, L.F., Ott, H.C., 2014. Decellularized scaffolds as a platform for bioengineered organs. Curr. Opin. Organ Transplant. 19, 145–152.
Tran, N.M.-p., Nguyen, D.T., Dai Luong, T., Bui, N.H., Van Toi, V., Nguyen, T.-H., 2018. Decellularization of bovine cancellous bone for bone tissue engineering application. In: International Conference on the Development of Biomedical Engineering in Vietnam. Springer, pp. 139–142.
Varettas, K., Taylor, P., 2011. Bioburden assessment of banked bone used for allografts. Cell Tissue Bank. 12, 37–43.
Varol, C., Mildner, A., Jung, S., 2015. Macrophages: development and tissue specialization. Annu. Rev. Immunol. 33, 643–675.
Vickers, N.J., 2017. Animal communication: when i'm calling you, will you answer too? Curr. Biol. 27, R713–R715.
Walsh, M.C., Takegahara, N., Kim, H., Choi, Y., 2018. Updating osteoimmunology: regulation of bone cells by innate and adaptive immunity. Nat. Rev. Rheumatol. 14, 146–156.
Watari, S., Hayashi, K., Wood, J.A., Russell, P., Nealey, P.F., Murphy, C.J., Genetos, D.C., 2012. Modulation of osteogenic differentiation in hMSCs cells by submicron topographically-patterned ridges and grooves. Biomaterials 33, 128–136.
Weaver, J.D., Song, Y., Yang, E.Y., Ricordi, C., Pileggi, A., Buchwald, P., Stabler, C.L., 2015. Controlled release of dexamethasone from organosilicone constructs for local modulation of inflammation in islet transplantation. Tissue Eng. Part A 21, 2250–2261.
Wessing, B., Lettner, S., Zechner, W., 2018. Guided bone regeneration with collagen membranes and particulate graft materials: a systematic review and meta-analysis. Int. J. Oral Maxillofac. Implants 33, 87–100.
You, L., Weikang, X., Lifeng, Y., Changyan, L., Yongliang, L., Xiaohui, W., Bin, X., 2018. In vivo immunogenicity of bovine bone removed by a novel decellularization protocol based on supercritical carbon dioxide. Artif. Cells Nanomed. Biotechnol. 46, 334–344.
You, P., Liu, Y., Wang, X., Li, B., Wu, W., Tang, L., 2020. Acellular pericardium: a naturally hierarchical, osteoconductive and osteoinductive biomaterial for guided bone regeneration. J. Biomed. Mater. Res. Part A.
Yu, Y., Cui, H., Zhang, C., Zhang, D., Yin, J., Wen, G., Chai, Y., 2020. Human nail bed extracellular matrix facilitates bone regeneration via macrophage polarization mediated by the JAK2/STAT3 pathway. J. Mater. Chem. B 8, 4067–4079.
Zheng, Z.-w., Chen, Y.-h., Wu, D.-y., Wang, J.-b., Lv, M.-m., Wang, X.-s., Sun, J., Zhang, Z.-Y., 2018. Development of an accurate and proactive immunomodulatory strategy to improve bone substitute material-mediated osteogenesis and angiogenesis. Theranostics 8, 5482.